

## Review

# Theranostics – a sure cure for cancer after 100 years?

Yangmeihui Song<sup>1,2#</sup>, Jianhua Zou<sup>3,4,5,6#</sup>, E. Alejandro Castellanos<sup>7#</sup>, Naomi Matsuura<sup>8,9,10</sup>, John A. Ronald<sup>11,12</sup>, Adam Shuhendler<sup>13,14</sup>, Wolfgang A Weber<sup>1,✉</sup>, Assaf A. Gilad<sup>15,16,✉</sup>, Cristina Müller<sup>17,18,✉</sup>, Timothy H. Witney<sup>19,✉</sup>, Xiaoyuan Chen<sup>3,4,5,6,✉</sup>

1. Department of Nuclear Medicine, Klinikum Rechts der Isar, Technical University of Munich, Munich, 81675, Germany.
2. Department of Nuclear Medicine, Union Hospital, Tongji Medical College, Huazhong University of Science and Technology, Wuhan, 43000, China.
3. Departments of Diagnostic Radiology, Surgery, Chemical and Biomolecular Engineering, and Biomedical Engineering, Yong Loo Lin School of Medicine and College of Design and Engineering, National University of Singapore, Singapore, 119074, Singapore.
4. Clinical Imaging Research Centre, Centre for Translational Medicine, Yong Loo Lin School of Medicine, National University of Singapore, Singapore 117599, Singapore.
5. Nanomedicine Translational Research Program, Yong Loo Lin School of Medicine, National University of Singapore, Singapore 117597, Singapore.
6. Institute of Molecular and Cell Biology, Agency for Science, Technology, and Research (A\*STAR), 61 Biopolis Drive, Proteos, Singapore, 138673, Singapore.
7. Department of Biomedical Engineering, Michigan State University, East Lansing, MI, USA.
8. Institute of Biomedical Engineering, University of Toronto, Toronto, ON, Canada.
9. Department of Materials Science & Engineering, University of Toronto, Toronto, ON, Canada.
10. Department of Medical Imaging, University of Toronto, Toronto, ON, Canada.
11. Imaging Laboratories, Department of Medical Biophysics, Robarts Research Institute, University of Western Ontario, London, ON, Canada.
12. Lawson Health Research Institute, London, ON, Canada.
13. University of Ottawa Heart Institute, Ottawa, ON, Canada.
14. Department of Chemistry and Biomolecular Sciences, University of Ottawa, Ottawa, ON, Canada.
15. Department of Chemical Engineering and Materials Sciences, Michigan State University, East Lansing, MI, USA.
16. Department of Mechanical Engineering, Michigan State University, East Lansing, MI, USA.
17. Center for Radiopharmaceutical Sciences, Paul Scherrer Institute, 5232 Villigen-PSI, Switzerland.
18. Department of Chemistry and Applied Biosciences, ETH Zurich, 8093 Zurich, Switzerland.
19. School of Biomedical Engineering & Imaging Sciences, King's College London, London, UK.

# These authors contribute equally to this work.

✉ Corresponding authors: Wolfgang A Weber (w.weber@tum.de), Assaf A. Gilad (gilad@msu.edu), Cristina Müller (cristina.mueller@psi.ch), Timothy H. Witney (tim.witney@kcl.ac.uk), Xiaoyuan Chen (chen.shawn@nus.edu.sg).

© The author(s). This is an open access article distributed under the terms of the Creative Commons Attribution License (<https://creativecommons.org/licenses/by/4.0/>). See <http://ivyspring.com/terms> for full terms and conditions.

Received: 2024.03.27; Accepted: 2024.03.28; Published: 2024.03.31

## Abstract

Cancer has remained a formidable challenge in medicine and has claimed an enormous number of lives worldwide. Theranostics, combining diagnostic methods with personalized therapeutic approaches, shows huge potential to advance the battle against cancer. This review aims to provide an overview of theranostics in oncology: exploring its history, current advances, challenges, and prospects. We present the fundamental evolution of theranostics from radiotherapeutics, cellular therapeutics, and nanotherapeutics, showcasing critical milestones in the last decade. From the early concept of targeted drug delivery to the emergence of personalized medicine, theranostics has benefited from advances in imaging technologies, molecular biology, and nanomedicine. Furthermore, we emphasize pertinent illustrations showcasing that revolutionary strategies in cancer management enhance diagnostic accuracy and provide targeted therapies customized for individual patients, thereby facilitating the implementation of personalized medicine. Finally, we describe future perspectives on current challenges, emerging topics, and advances in the field.

Keywords: cancer, radiotheranostics, synthetic biology, nanotheranostics, personalized medicine

## Introduction

In 1998, the Chief Executive Officer of PharmaNetics, John Funkhouser, coined the term “Theranostics” or “Theragnostics” to describe his company's business model in developing diagnostic

tests directly linked to the applying specific therapies [1]. Theranostics is commonly defined as a combination of imaging and therapy, both using the same target. This combination promises to create a

paradigm shift in individual cancer patient care through an optimized treatment strategy. Personalization is achieved through the addition of the companion diagnostic test, which enables the identification of patients who would most likely profit or – in the case of a negative diagnostic outcome – be harmed by targeted drug therapy.

With biomedical research's flourishing and unprecedented progress, over 20,000 articles on theranostics have been published in the past decade. Theranostics is presently employed in a broad context, integrating molecularly targeted imaging and therapy to provide actionable information for the development of novel or more efficacious therapeutic interventions [2]. Radiotheranostics and nanotheranostics, the most representative and influential domains within the expansive field of theranostics, harness the power of radiopharmaceuticals and nanoparticles (NPs), respectively, to revolutionize disease diagnosis, monitoring, and treatment. With the rapid advancement of synthetic biology, theranostics has also gained new opportunities to expand its toolkit. Together, these approaches enable precise targeting and delivery of therapeutic agents to the tumor tissue while concurrently providing real-time imaging and assessment of treatment efficacy, ushering in a new era of personalized medicine and transformative advancements in healthcare.

In this review, we will focus on radiotheranostics, including a brief introduction of the history and several typical examples currently employed in clinical trials. In addition, we will introduce nanotheranostics, which benefits from multiple advantages of nanomaterials such as rational design and easy modification, which will encompass photo-, chemo-, immuno-, and sonotheranostics. Due to the disconnection between the papers published and their clinical application, the disadvantages, and prospects of theranostics have been described. We hope this review could offer a comprehensive view of the opportunities and challenges faced by the field of theranostics, providing some insights for future researchers.

## Radiotheranostics

### Historical overview

The concept of radiotheranostics was hinted at as early as 1921 by the famous Marie Curie, who was convinced that radium could serve as a sure cure for cancer even in deeply rooted cases if properly treated. However, Vassar Smith, a prominent member of the American Chemical Society and Academy of Sciences, warned that radium is not a panacea for all types of cancer. At that time, the concept was not universally

acknowledged due to the lack of clinical trials. Two decades later, in 1946, Saul Hertz and Samuel Seidlin pioneered the use of iodide-131 to treat hyperthyroidism and thyroid adenocarcinoma metastases, signaling the advent of radiotheranostics [3, 4]. The resulting improvement in treated patients was such that in 1951 the United States Food and Drug Administration (FDA) approved the use of iodide-131 for thyroid cancer treatment. The exclusive emission of  $\gamma$ -radiation by iodide-123 meant that employing iodide-123 imaging prior to iodide-131 therapy could aid treatment planning. As a result, the combination of iodide-123 and iodide-131 became the first pair of diagnostic and therapeutic radioisotopes harnessed in radiotheranostics [5]. This milestone underlined the practical application and clinical exploration of radiotheranostics. Thereafter, the use of [ $^{111}\text{In}$ ]In-octreotide in 1982 triggered extensive interest in radiotheranostics for neuroendocrine neoplasms (NENs). Whilst these two examples showcased the opportunity for radiotheranostics to provide precision treatment of disease, it is only recently that its potential has started to be realized.

Over the past decade, there has been unprecedented progress in the field of theranostics through the development and application of targeted radionuclide therapies. The FDA's approval of [ $^{68}\text{Ga}$ ]Ga-DOTATATE positron emission tomography (PET)/CT and [ $^{177}\text{Lu}$ ]Lu-DOTATATE in 2016 and 2018 for the diagnosis and treatment of NETs, respectively, and the approval of [ $^{68}\text{Ga}$ ]Ga-PSMA-11 and [ $^{177}\text{Lu}$ ]Lu-PSMA-617 in 2022 for the diagnosis and treatment of prostate cancer, respectively, marked a turning point in the perception of nuclear medicine in the wider community. These successful cases have substantially raised the profile of this once-limited imaging technology in oncology and attracted considerable attention from various medical fields and industrial backing [6]. The clinical significance of radiotheranostics for cancer, particularly for refractory advanced-stage cases, is now evident, supported by extensive explorations and breakthroughs.

### Principles of radiotheranostics

Of all categories of theranostics, radiotheranostics is the only one that has integrated into clinical practice. It refers to the amalgamation of radionuclide imaging and radionuclide therapy, as presented above for [ $^{123}\text{I}$ ]iodide and [ $^{131}\text{I}$ ]iodide, or for targeted radiopharmaceuticals based on identical or similar compounds labeled with either diagnostic or therapeutic radionuclides (Figure 1). Radiopharmaceuticals are composed of variable structural components, including entities for specific

receptor/enzyme targeting, linkers as pharmacokinetic modifiers, and chelators for coordination of the radionuclides. Radionuclides are classified as either diagnostic or therapeutic based on their emitted radiation. Radionuclides that emit  $\gamma$ -radiation or  $\beta^+$ -particles are useful for imaging purposes, while those that emit  $\beta^-$  or  $\alpha$ -particles and/or Auger electrons can be used for therapy. Certain radionuclides, like lutetium-177 and holmium-166, which are primarily utilized for therapeutic purposes because they emit therapeutic  $\beta^-$ -particles, can also facilitate post-therapy imaging and dosimetry through their concomitant emission of  $\gamma$ -rays, though they are not generally used for diagnostic imaging.

Considering diagnostics as the ability to identify a disease and its state, theranostics provides the diagnostic capability with a direct impact on the applied therapy. Radiotheranostics employs nuclear imaging to confirm target engagement when selecting patients for radionuclide therapy.

**Table 1.** Radiopharmaceuticals for Radiotheranostics Recently Approved by the FDA

Name	Target	Classification	Indications	Approved Date
[ <sup>68</sup> Ga]Ga-DOTATATE (Netspot)	SSTR2	Diagnostics	NEN	June 2016
[ <sup>177</sup> Lu]Lu-DOTATATE (Lutathera)	SSTR2	Therapy	NEN	January 2018
[ <sup>68</sup> Ga]Ga-DOTATOC	SSTR2 > 5	Diagnostics	NEN	August 2019
[ <sup>64</sup> Cu]Cu-DOTATATE (Detectnet)	SSTR2	Diagnostics	NEN	September 2020
[ <sup>68</sup> Ga]Ga-PSMA-11 (Locametz)	PSMA	Diagnostics	Prostate cancer	December 2020
[ <sup>18</sup> F]F-DCFPyL (Pylarify)	PSMA	Diagnostics	Prostate cancer	May 2021
[ <sup>68</sup> Ga]Ga-PSMA-617	PSMA	Diagnostics	Prostate cancer	March 2022
[ <sup>177</sup> Lu]Lu-PSMA-617 (Pluvicto)	PSMA	Therapy	Prostate cancer	March 2022
[ <sup>18</sup> F]F-rhPSMA-7.3 (Posluma)	PSMA	Diagnostics	Prostate cancer	May 2023

SSTR: somatostatin receptor; NEN: neuroendocrine neoplasm; PSMA: prostate-specific membrane antigen.

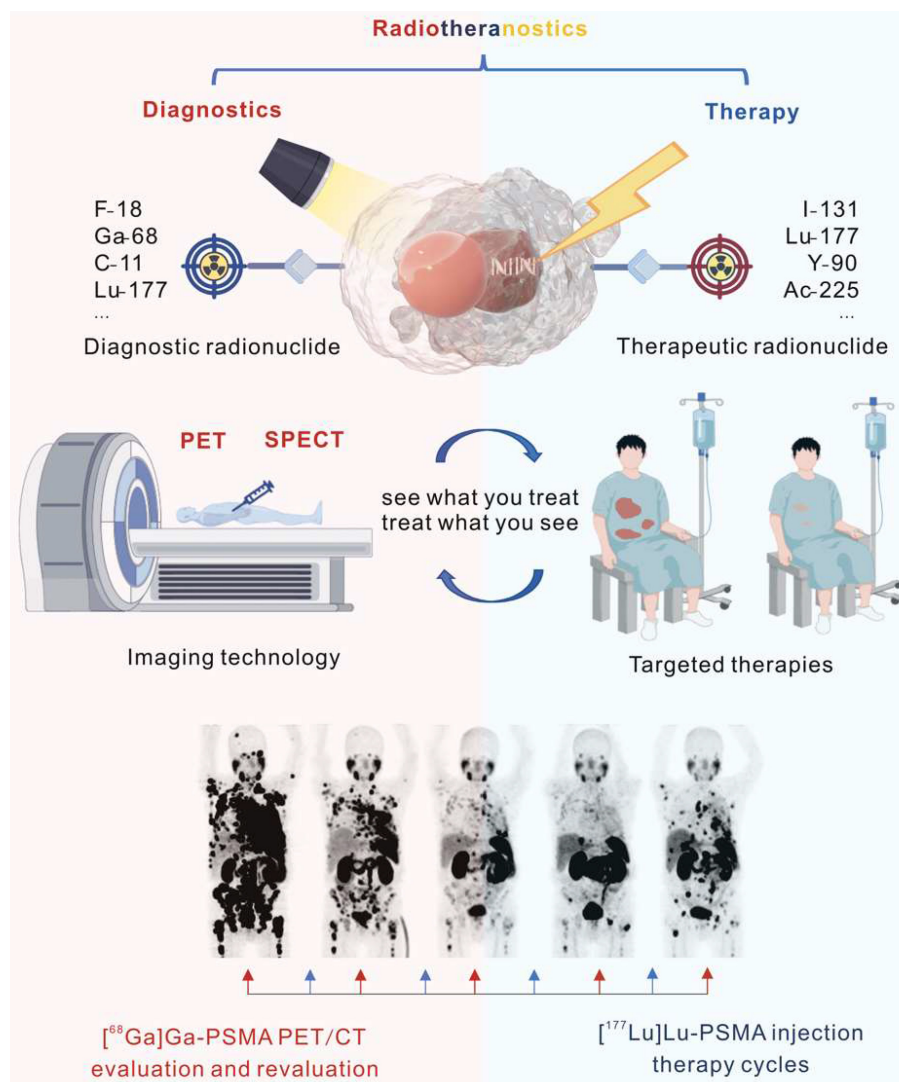


**Figure 1.** Illustration of radiotheranostics. Adapted with permission from [195], Copyright 2023 Springer Nature.

Moreover, nuclear imaging allows for accurate estimation of tumor dosimetry, which could facilitate personalized and optimized therapeutic interventions. In contrast to other targeted treatment modalities, the heterogeneous target expression, which is often the case in the tumor mass, is less problematic for radionuclide therapy because it only necessitates a few bound molecules to destroy the target cells. Moreover, in the case of  $\beta^-$ -particles, the range of the employed radiation extends to neighboring cancer cells, resulting in cell death even if the target is not widely expressed. Utilizing only microgram amounts of substances, usually without any pharmacological effects, also minimizes the risk of unexpected off-target toxicity.

### Current clinical research advances

#### Radiopeptides for somatostatin receptor-targeting radiopharmaceuticals

NENs, predominantly found in the gastrointestinal tract, pancreas, and lungs, are a diverse group of tumors that originate from neuroendocrine cells, which often overexpress somatostatin receptors (SSTRs), in particular SSTR2. At present, a variety of somatostatin analogs, including SSTR agonists are available for clinical and experimental purposes. The most widely used SSTR-targeting peptides include three types of somatostatin agonists, namely Tyr<sup>3</sup>-octreotide (TOC), D-Phe<sup>1</sup>-Tyr<sup>3</sup>-Thr<sup>8</sup>-octreotide (TATE), and Nal<sup>3</sup>-octreotide (NOC). These three peptides, derivatized with a DOTA chelator (DOTATOC, DOTATATE, and DOTANOC, respectively) and labeled with a diagnostic or therapeutic radionuclide, have slightly different pharmacokinetic profiles due to differing affinities for SSTR subtypes. These radiopeptides, however, exhibit comparable accuracy for lesion detection using SSTR PET, and superiority over scintigraphy or conventional imaging methodology such as computer tomography (CT) [7]. Initially leveraging indium-111 for imaging and yttrium-90 for early therapy, the field has now shifted towards the use of lutetium-177, favored for lutetium-177's ideal penetration depth, making it more effective at targeting micrometastases in NENs. The NETTER-1 Phase III clinical trial stands as a groundbreaking randomized controlled trial that has effectively demonstrated the efficacy and safety of theranostics utilizing [<sup>177</sup>Lu]Lu-DOTATATE [8]. In this trial, patients with metastatic well-differentiated midgut NENs treated with [<sup>177</sup>Lu]Lu-DOTATATE and best supportive care showed a remarkable estimated progression-free survival (PFS) rate of approximately 65.2% at the 20<sup>th</sup> month, significantly higher than the 10.8% in the control group receiving only octreotide. Furthermore, the study not only

demonstrated a decrease in mortality (14 *vs.* 26 months) and a 60% reduction in the risk of death within the [<sup>177</sup>Lu]Lu-DOTATATE group but also established an acceptable safety profile with manageable hematologic toxicity. Then, the clinical trial (NCT01456078) based on renal dosimetry confirmed the low toxicity and promising efficacy of [<sup>177</sup>Lu]Lu-DOTATATE treatment [9]. Following the release of these results, Novartis capitalized on the recognized significance of peptide receptor radionuclide therapy (PRRT) by acquiring Advanced Accelerator Applications for \$3.9 billion, gaining access to its primary product, Lutathera™ ([<sup>177</sup>Lu]Lu-DOTATATE), which was subsequently endorsed as a treatment option by the European Neuroendocrine Tumor Society in their guidelines [10].

The use of SSTR antagonists in radiotheranostics has been explored despite the initial belief that radiopeptides were required to be internalized into cancer cells to be effective, as is the case for SSTR agonists (Figure 2A and Figure 2B). In 2006, Ginj *et al.* first demonstrated that the SSTR antagonists, [<sup>111</sup>In]In-DOTA-sst3-ODN-8 and [<sup>111</sup>In]In-DOTA-sst2-ANT, exhibited superior performance in mice bearing SSTR3- and SSTR2-expressing tumors even in the absence of internalization [11]. Subsequently, the clinical feasibility of imaging NETs with [<sup>111</sup>In]In-DOTA-BASS and [<sup>68</sup>Ga]Ga-DOTA-JR11 ([<sup>68</sup>Ga]Ga-Satoreotide Tetraxetan) has been established, producing high tumor/background ratios and sensitivity [12, 13]. This has given rise to the viewpoint that SSTR antagonists may improve diagnostic accuracy and therapy when labeled with therapeutic radionuclides [14, 15]. The first Phase I trial evaluating the efficacy of [<sup>177</sup>Lu]Lu-DOTA-JR11 in 20 patients with advanced SSTR2-positive NETs revealed a sustained partial response, with an overall response rate of 45%, including a 5% complete response, 40% partial response, and 40% stable disease rate [16].

#### Radioligands for PSMA-targeting radiopharmaceuticals

The prominent role of radiotheranostics in managing NET patients is paralleled by radiotheranostic interventions in prostate cancer patients. The prostate-specific membrane antigen (PSMA), an enzyme expressed on the surface of prostate cancer cells, plays a crucial role in prostate cancer progression by modulating the phosphoinositide 3-kinase (PI3K) pathway and glutamine production [17, 18]. Since 2012, PSMA-targeting radioligands based on low-molecular-weight peptidomimetics have shown the capability to image PSMA-expressing prostate cancer [19, 20]. [<sup>68</sup>Ga]Ga-PSMA-11 PET

images provided excellent contrast as early as 1 h after injection of the radioligand with high detection rates of prostate cancer lesions even at low prostate-specific antigen (PSA) levels [21]. Next, Zechmann *et al.* demonstrated that radioligand therapy using the PSMA-targeting small molecule  $^{124}\text{I}/^{131}\text{I}$ -MIP-1095 enabled unprecedented doses delivered to the tumor lesions. Indeed, the absorbed doses in the involved lymph nodes and bone metastases exceed 300 Gy [22]. Following this, Heck *et al.* observed a median clinical PFS of 4.1 months and a median overall survival of 12.9 months in 100 metastatic castration-resistant prostate cancer (mCRPC) patients undergoing 319 cumulative cycles of  $^{177}\text{Lu}$ Lu-PSMA-I&T treatment [23]. Clinical trials have consistently demonstrated biochemical response after radioligand therapy with  $^{177}\text{Lu}$ Lu-PSMA-617/I&T, whose results demonstrated a reduction in PSA levels of 50% or more, with response rates ranging from 32.2% to 66% [23–29]. The VISION trial was the first to demonstrate a survival benefit of  $^{177}\text{Lu}$ Lu-PSMA-617 in combination with standard of care, with improved radiographic PFS (8.7 months *vs.* 3.4 months) and overall survival (15.3 months *vs.* 11.3 months) compared to standard of care alone in 831 PSMA-positive mCRPC patients [27]. Then, FDA approval of  $^{177}\text{Lu}$ Lu-PSMA-617 (Pluvicto™) and  $^{68}\text{Ga}$ Ga-PSMA-11 (Locametz™) for

mCRPC resulted in further industry interest in nuclear medicine treatment and integration of diagnostics. Ongoing trials, such as multicenter PSMAfore (NCT04689828) and global PSMAAddition (NCT04720157), are investigating the efficacy and safety of  $^{177}\text{Lu}$ Lu-PSMA-617 in mCRPC and metastatic hormone-sensitive prostate cancer patients, with the hope that these trials will provide further evidence of the potential of radiotherapeutics as a novel therapeutic strategy which is applied in conjunction with the diagnostic match.

Conventional imaging methods such as CT and magnetic resonance imaging (MRI) have limitations in identifying recurrence in patients with low PSA levels.  $^{68}\text{Ga}$ Ga-PSMA ligand PET imaging has shown promise to improve the detection rates of recurrent prostate cancer (Figure 2C) [30]. A cohort of 272 consecutive patients imaged with  $^{68}\text{Ga}$ Ga-PSMA-11 PET showed detection rates for patients with very low PSA levels (0.2–0.5 ng/mL) and values >0.5–1.0 ng/mL were 55% and 74%, respectively [31]. Consequently, PET/CT scans using  $^{68}\text{Ga}$ Ga-PSMA-11 demonstrated the potential for restaging in cases of recurrent prostate cancer [32]. Furthermore, PSMA-radio-guided surgery is a viable option for oligometastatic lesions, allowing for salvage surgery to be precisely conducted under the direction of an

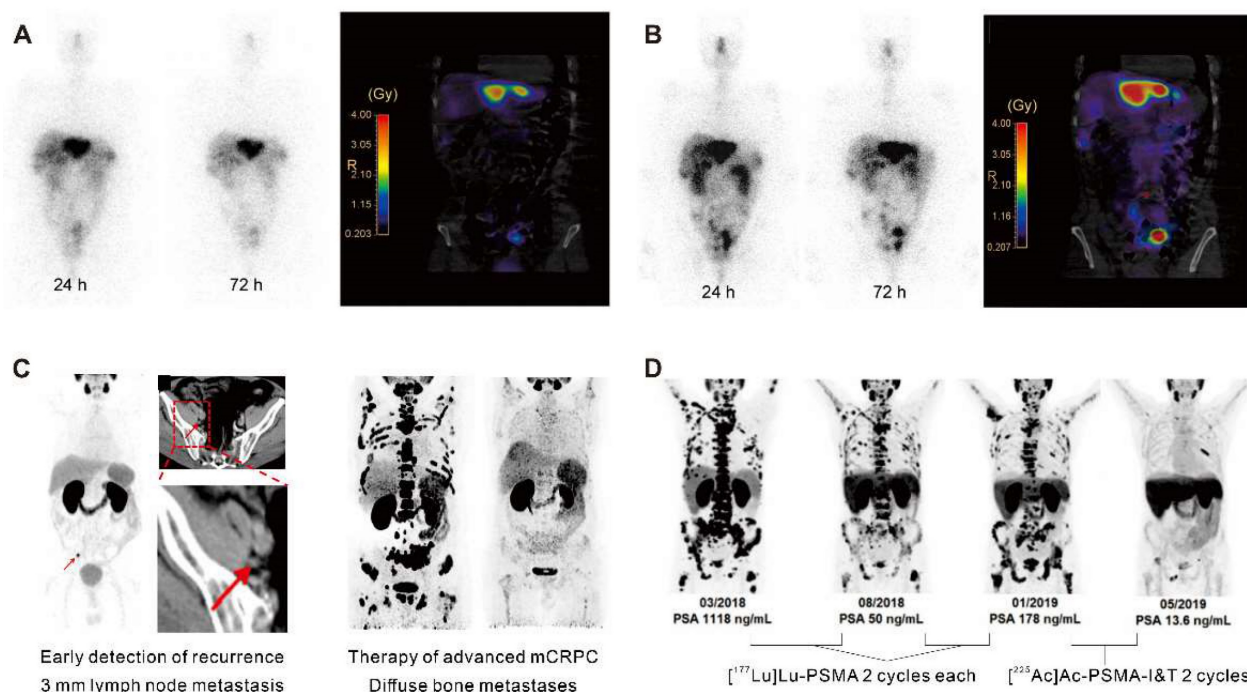


**Figure 2.** Clinical application in radiotheranostics. A.  $^{177}\text{Lu}$ Lu-DOTATATE planar scans (left) and isodose curves (right) of a patient with G2 neuroendocrine tumor (ileum) after injection of  $^{177}\text{Lu}$ Lu-DOTATATE. B. Corresponding  $^{177}\text{Lu}$ Lu-DOTA-JR11 planar scans (left) and isodose curves (right) after injection of  $^{177}\text{Lu}$ Lu-DOTA-JR11. Adapted with permission from [15], Copyright 2014 Society of Nuclear Medicine and Molecular Imaging. C. A 75-year-old post-radical prostatectomy patient exhibited intense uptake on  $^{68}\text{Ga}$ Ga-PSMA PET, indicating a single lymph node metastasis confirmed by biopsy (left); a 58-year-old patient with mCRPC showed multiple systemic metastases in baseline and significant improvement in post-treatment  $^{68}\text{Ga}$ Ga-PSMA-11 PET/CT after  $^{177}\text{Lu}$ Lu-PSMA-I&T therapy (right). Adapted with permission from [29, 30], Copyright 2015 Society of Nuclear Medicine and Molecular Imaging and 2022 Frontiers Media S.A. D. A 79-year-old mCRPC patient responded to initial  $^{177}\text{Lu}$ Lu-PSMA treatment but experienced disease progression, showing a significant response to subsequent  $^{225}\text{Ac}$ Ac-PSMA-I&T therapy. Adapted with permission from [39], Copyright 2014 Society of Nuclear Medicine and Molecular Imaging.

intraoperative  $\gamma$  probe after intravenous application of [ $^{99m}\text{Tc}$ ]Tc-PSMA-I&S investigation and surgery. This method has been substantiated as valuable and safe for accurately identifying and removing metastatic lesions, as demonstrated in an initial trial of 31 consecutive patients. Evaluated on a specimen basis, the radioactive rating demonstrated a sensitivity of 83.6%, a specificity of 100%, and an accuracy of 93.0% [33]. Following this, 121 consecutive patients diagnosed with recurrent prostate cancer via PSMA-ligand PET underwent PSMA-radioguided surgery, successfully resecting metastatic tissue in almost all patients (120/121, 99%). In this cohort, 66% of patients achieved a complete biochemical response. Particularly, those with lower preoperative PSA levels and a solitary lesion on PET using PSMA-targeting radioligands exhibited complete biochemical response (84%) and biochemical recurrence-free survival (median, 19.8 months) [34].

In a further development, Wurzer *et al.* invented a series of  $^{18}\text{F}$ -labeled PSMA-targeted inhibitors with excellent labeling and production properties, named radiohybrid PSMA inhibitors (rhPSMAs). Such rhPSMA ligands can be labeled with  $^{18}\text{F}$ , whereas the chelator is used for the complexation of a cold metal (like  $^{\text{nat}}\text{Ga}$  or  $^{\text{nat}}\text{Lu}$ ) or can be labeled with a radiometal (like gallium-68, lutetium-177, or actinium-225), keeping the fluorine side nonradioactive with  $^{19}\text{F}$ . Preclinical studies demonstrated that these radiotracers had a high affinity for PSMA-expressing cells, efficient internalization, low lipophilicity, and strong binding to human serum albumin (HSA). They displayed high tumor uptake, rapid clearance kinetics, minimal hepatobiliary excretion, and low bone uptake, making them ideal candidates as prostate cancer theranostics [35]. Based on this encouraging preclinical data, the development of rhPSMA7.3, an imaging agent for prostate cancer, has rapidly progressed from preclinical evaluation to Phase 3 clinical trials within a remarkably short three years. After this rapid development, the agent [ $^{18}\text{F}$ ]F-rhPSMA-7.3 has now garnered approval from the FDA. In preclinical evaluation, [ $^{19}\text{F}$ ]F/[ $^{177}\text{Lu}$ ]Lu-rhPSMA-7.3 showed a 2.6-fold higher initial tumor uptake and longer retention compared to [ $^{177}\text{Lu}$ ]Lu-PSMA-I&T. In comparison to [ $^{177}\text{Lu}$ ]Lu-PSMA I&T, [ $^{19}\text{F}$ ]F/[ $^{177}\text{Lu}$ ]Lu-rhPSMA-7.3 emerged as a viable candidate for clinical translation, given its analogous clearance kinetics and comparable radiation dosage to healthy organs, combined with enhanced tumor uptake and retention. Furthermore, PET/CT using [ $^{18}\text{F}$ ]F-rhPSMA-7 has shown exceptional detection rates in early biochemical recurrence after radical prostatectomy, with pathological findings observed in 81% of patients and detection rates reaching 95% at

PSA levels of  $\geq 2$  ng/mL, irrespective of prior therapy or primary Gleason score [36].

The application of radiotheranostics in prostate cancer has been explored in a broader context. Kratochwil *et al.* reported low liver and kidney damage in a cohort study of 30 mCRPC patients treated with [ $^{177}\text{Lu}$ ]Lu-PSMA-617. Bone marrow toxicity was minimal and mainly observed in patients with extensive bone marrow metastasis [24]. A retrospective study of [ $^{177}\text{Lu}$ ]Lu-PSMA-617 in 145 mCRPC patients demonstrated acceptable safety, with 12% experiencing grade 3-4 bone marrow suppression, 8% developing radiogenic oral pain, and 6% exhibiting symptoms of nausea [25]. Gafita *et al.* found that patients with extensive bone marrow involvement showed comparable safety and efficacy to previous studies, suggesting that patients with unusually intense and uniform uptake in the skeletal system, a so-called “superscan”, should not be excluded [37]. They also developed and externally validated nomograms based on clinicopathological and imaging variables to predict outcomes following [ $^{177}\text{Lu}$ ]Lu-PSMA-617 therapy, guiding clinical trial design and individual decision-making [38]. The TheraP study (NCT03392428) was the first clinical trial to compare [ $^{177}\text{Lu}$ ]Lu-PSMA-617 and cabazitaxel treatments in mCRPC patients who had progressed after docetaxel, showing that treatment with [ $^{177}\text{Lu}$ ]Lu-PSMA-617 significantly increased the PSA<sub>50</sub> response rate (66% *vs.* 37%) and had a lower incidence of adverse events (33% *vs.* 53%) compared to cabazitaxel. However, after a three-year follow-up, there was no significant difference in overall survival between the two groups [26].

The choice of radionuclide has important implications for therapeutic efficacy. Alpha particles have a shorter tissue range but a considerably higher linear energy transfer (LET; 50-230 keV), hence, they are more potent to induce cytotoxicity than  $\beta^-$ -particles emitted by lutetium-177. Tumor-targeted  $\alpha$ -therapy demonstrated significant antitumor effects in advanced mCRPC patients refractory to  $^{177}\text{Lu}$ -based radioligand therapy. In patients with advanced mCRPC who had previously received treatment with [ $^{177}\text{Lu}$ ]Lu-PSMA, [ $^{225}\text{Ac}$ ]Ac-PSMA-617 and [ $^{225}\text{Ac}$ ]Ac-PSMA-I&T demonstrated comparable antitumor efficacy (Figure 2D) [39]. The median time to progression of PSA with [ $^{225}\text{Ac}$ ]Ac-PSMA-617 therapy was 3.5 months, clinical PFS was 4.1 months, and overall survival was 7.7 months. However, a substantial portion of patients experienced grade 3/4 hematological adverse events, and a quarter of patients discontinued treatment due to irreversible xerostomia due to the high-energy and short-range nature of  $\alpha$ -nuclide therapy [40]. This may be related

to the inherent high energy and limited penetration depth of the alpha nuclides and their daughter isotopes.

### New radiotheranostics targets

C-X-C-motif chemokine receptor 4 (CXCR4) is a crucial receptor for the chemokine stromal cell-derived factor-1 involved in the development, chemotaxis, and metastasis of various tumor types, including pancreatic, breast, lung, prostate, and colorectal cancers. Although meaningful data on CXCR4 targeting in solid tumors remains elusive to date, recent advancements have introduced radio-labeled CXCR4 ligands, such as [<sup>68</sup>Ga]Ga-Pentixafor or [<sup>177</sup>Lu]Lu-Pentixather. These ligands have shown favorable results as *in vivo* theranostics for advanced multiple myeloma (Figure 3A) [41, 42] and as a pre-treatment strategy before autologous stem cell transplantation in advanced diffuse large B-cell lymphoma, often in combination with conventional chemotherapy regimens [43].

Fibroblast activation protein (FAP) is highly overexpressed in cancer-associated fibroblasts that are present within the tumor microenvironment. These cancer-associated fibroblasts play a pivotal role in tumor growth, invasiveness, and immune suppression [44]. Benefiting from minimal expression in normal tissues but excessive expression in epithelial tumors, FAP is an attractive target for cancer theranostics. Antibody-based FAP-targeted radiopharmaceuticals like [<sup>89</sup>Zr]Zr/[<sup>177</sup>Lu]Lu-AMS002-1-Fc rAb and FAP inhibitor (FAPI) radiopharmaceuticals such as [<sup>211</sup>At]At/[<sup>225</sup>Ac]Ac-FAPI-04 and [<sup>177</sup>Lu]Lu/[<sup>225</sup>Ac]Ac-FAPI-46 have demonstrated tumor growth suppression in preclinical models [45-47]. In clinical trials, [<sup>90</sup>Y]Y-FAPI-04/46 has exhibited good tolerance and effective alleviation of cancer-related pain [48,

49]. The eagerly anticipated peptide-based FAP-targeted therapeutic drug, FAP-2286, and the highly selective peptide, PNT6555 is currently undergoing further clinical evaluation [NCT04939610 (LuMIERE) and NCT05432193 (FRONTIER)] owing to their outstanding preclinical dose-dependent anti-tumor effects and initial clinical feasibility (Figure 3B) [50-52]. Furthermore, two Phase I clinical trials utilizing [<sup>177</sup>Lu]Lu-LNC1004 (NCT05723640) and [<sup>177</sup>Lu]Lu-EB-FAPI (NCT05400967) targeting FAP are also of interest. These studies indicate the significant potential for FAP-targeted radiotheranostics in the treatment of various types of cancer, with ongoing clinical trials likely to provide further insights.

### Principal challenges and improved strategies in radiotheranostics

As a paradigm of radiotheranostics, the successful applications of iodide-131 and the sodium iodide symporter in thyroid cancer fortuitously met all the requirements for a successful anti-cancer therapy. Repeating the success of radioiodine therapy requires extensive biological, pharmacological, and medical research. Firstly, high affinity (< 10 nM) ligands with sufficient target specificity are required, which is easily influenced by the coordinated radiometal. For instance, the affinity of SSTR2 agonist [<sup>68</sup>Ga]Ga-DOTATATE and antagonist [<sup>68</sup>Ga]Ga-DOTA-JR11 for the receptor differs markedly, exhibiting IC<sub>50</sub> values of 0.2 nM and 29.0 nM, respectively as antagonists are highly sensitive to N-terminal modifications of the peptide chain. This discrepancy is inverted when the peptides are labeled with lutetium-177, displaying IC<sub>50</sub> values of 2.7 nM and 0.7 nM for [<sup>177</sup>Lu]Lu-DOTATATE and [<sup>177</sup>Lu]Lu-DOTA-JR11, respectively [53, 54]. Moreover, minor modifications of the ligand structure

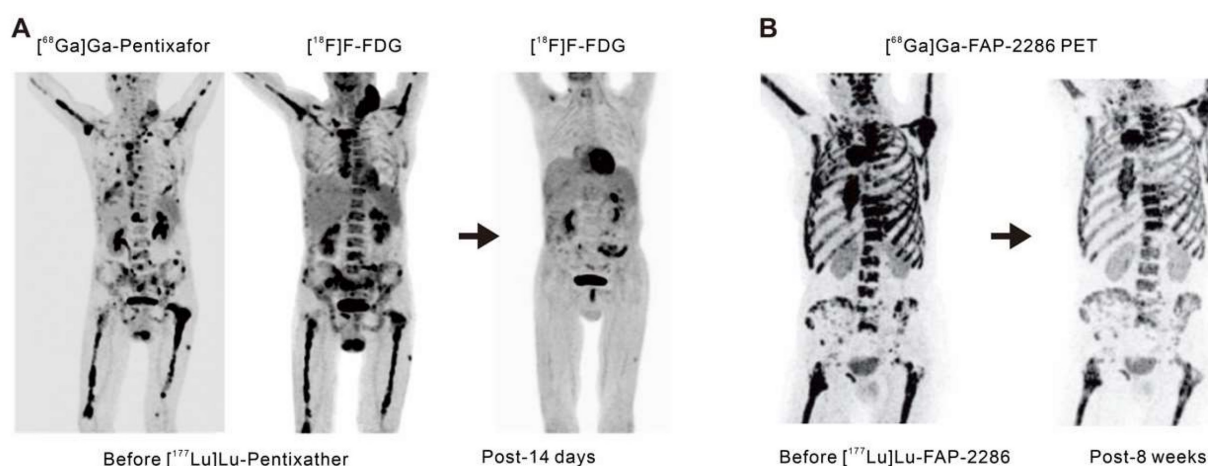


**Figure 3.** Advancements in radiotheranostics targeting novel biomarkers. A. Targeting the chemokine CXCR4 with Pentixafor/Pentixather. Adapted with permission from [42], Copyright 2023 Society of Nuclear Medicine and Molecular Imaging. B. Initial results of peptide-receptor radionuclide therapy with [<sup>177</sup>Lu]Lu-FAP-2286. Adapted with permission from [50], Copyright 2022 Society of Nuclear Medicine and Molecular Imaging.

may drastically affect the affinity for peptides and small molecules. For example, a change in the chelator of JR11 from DOTA to NODAGA resulted in a decrease in  $IC_{50}$  value from 29 nM to 1.2 nM [54]. Furthermore, sufficient metabolic stability of the radiopeptide *in vivo* is also a crucial factor that may substantially influence tissue distribution. Radioiodination of FAPI-01 provides an example of *in vivo* instability due to the time-dependent enzymatic deiodination of [ $^{125}I$ ]I-FAPI-01, resulting in decreased intracellular radioactivity over time [55].

An optimal radionuclide therapy is based on high accumulation and retention of the radiation source in the tumor tissue. At the same time, minimal uptake of a radiopharmaceutical in non-targeted organs is important, particularly in radiation-sensitive tissues such as the bone marrow, due to the risk of hematological toxicity, which must be avoided to safeguard the function of hematopoietic cells. The SSTR is not only a relevant theranostic target, but also plays a pivotal role as a selective chemoattractant for immature hematopoietic cells by activating multiple intracellular pathways [56, 57]. Precise dose management in order to optimize treatment outcomes is important while mitigating toxicities in NEN patients undergoing radiolabeled somatostatin antagonist therapy. In the Phase I trial of [ $^{177}Lu$ ]Lu-JR11 for the treatment of well-differentiated NENs, the red marrow dose was kept below 1.5 Gy, the kidney dose was kept under 23 Gy, and the administered activity did not exceed 7.4 GBq per cycle. Among the seven patients treated, four experienced Grade 4 hematological toxicity, which was resolved after adjustment of the injected activity and, consequently absorbed dose to the hematopoietic tissue [16]. In the future, the investigation of SSTR-related uptake by hematopoietic cells in the red bone marrow may provide valuable insights into the intricate interaction between SSTRs and hematopoietic cells.

The delicate balance of ensuring sufficient clearance of radiopharmaceuticals from blood circulation is critical. Insufficient clearance rates can potentially culminate in bone marrow toxicity, whereas excessively rapid clearance might compromise tumor uptake. In comparison to radioimmunoconjugates, which provide extended blood circulation and substantial tumor accumulation, small-molecular-weight radioligands are rapidly cleared by the kidneys, resulting in shorter residence times in blood circulation. However, given the numerous advantages of small molecule radioligands, including ease of production, cost-effectiveness, straightforward procedures for radiometallic conjugation, flexible chemical modifications, and adherence to Good

Manufacturing Practice standards, considerable research has been invested in devising strategies to augment the blood residence time of these radioligands. The strategies include the integration of targeted amino acid sequences, the removal of non-essential substituents, and the addition of functional units. Albumin, the predominant protein in human serum, may serve as an invaluable carrier for theranostic agents [58]. Conjugation with an albumin-binding entity is a commonly employed strategy to prolong the blood circulation time of small molecules and results in enhanced tumor uptake. Müller *et al.* first demonstrated the feasibility of conjugating an albumin binder to folate-based radioconjugates to improve tumor-to-kidney ratio and extend circulation time [59]. More groups have explored albumin-binding derivatives of PSMA-617, which incorporate a range of albumin-binding moieties, such as 4-(4-iodophenyl)butanoic acid [60, 61], 4-(4-chlorophenyl)butanoic acid [62], ibuprofen [63, 64], the moderate-affinity p-(tolyl)butanoic acid moiety [65, 66], and Evans Blue (EB) [67-69] (Figure 4). In the case of folate radioconjugates, an effective strategy to enhance the tumor uptake was the direct structural modification of the targeting moiety. Guzik *et al.* employed a class of albumin-binding radioconjugates comprising 5-methyltetrahydrofolate as a targeting agent, which exhibited a high tumor-to-kidney ratio, yielding superior therapeutic outcomes as compared with the unmodified [ $^{177}Lu$ ]Lu-labeled conjugates [72]. Synergistic optimization of this approach can be achieved through modifications in linkers [73, 74]. Incorporating a lipophilic linker proximal to the albumin binder subtly elevates the tumor-to-kidney ratios of the radioconjugates, while the employment of a hydrophilic linker attenuates albumin-binding capabilities, leading to suboptimal tumor-to-kidney ratios, as demonstrated with folate radioconjugates. Moreover, the charge and length of disparate linkers can significantly influence the pharmacokinetic properties of radioligands as demonstrated with PSMA radioligands [75, 76]. Kuo *et al.* synthesized [ $^{177}Lu$ ]Lu-HTK03121 with the tranexamic acid-9-anthryl alanine affinity-modifying group, exhibiting 18.7 times higher absorbed dose to the tumor compared to [ $^{177}Lu$ ]Lu-PSMA-617, but only a 6.4-fold increase in dose to the kidneys, improving the tumor-to-kidney dose ratio 3-fold [62]. Additionally, Borgna & Deberle *et al.* found that [ $^{177}Lu$ ]Lu-SibuDAB, which utilizes (S)-ibuprofen as the albumin binder, exhibited stronger plasma protein binding and metabolic stability than its analogue derivatized with (R)-ibuprofen (referred to as [ $^{177}Lu$ ]Lu-RibuDAB), further supporting the potential clinical translation of

[<sup>177</sup>Lu]Lu-SibuDAB [64]. The emergence of [<sup>177</sup>Lu]Lu-PSMA-ALB-56 with an albumin binder based on the p-(tolyl)-moiety has also been clinically evaluated (Figure 4C) [66]. Kramer *et al.* evaluated the safety and dosimetry of [<sup>177</sup>Lu]Lu-PSMA-ALB-56 in 10 mCRPC patients, showing improved blood circulation, higher absorbed doses in tumor lesions (2.3-fold), but significantly higher in kidney accumulation (8.2-fold) compared to PSMA-617 and PSMA I&T, hampering further clinical development (Figure 4A) [70]. Chen *et al.* conceptualized and devised a series of PSMA-617 derivatives attached to the EB derivatives. EB-PSMA-617 illustrated a comparable affinity to PSMA as PSMA-617 (IC<sub>50</sub> 13.7 nM *vs.* 15.4 nM), optimal internalization into tumor cells (80% *vs.* 44% at the 24 h time point), and prolonged tumor uptake [67]. A successive translational study involved nine mCRPC patients and revealed that [<sup>177</sup>Lu]Lu-EB-PSMA-617 not only presented increased tumor accumulation but also

demonstrated superior therapeutic outcomes compared with [<sup>177</sup>Lu]Lu-PSMA-617, even with a single imaging dose [68, 69]. Subsequently, a second-generation radioligand, LNC1003, was invented with enhanced pharmacokinetics and pharmacodynamics, showcasing significant potential for radiotheranostics in patients expressing moderate levels of PSMA and displaying exceptional metabolic stability (Figure 4B) [71, 72]. Additionally, [<sup>177</sup>Lu]Lu-DOTA-EB-TATE also achieved a favorable survival outcome in patients with NENs [73].

The selection of appropriate radionuclides is of paramount importance to maximize the efficacy of radiotheranostics. Radionuclides typically emit one (or more) of three distinct types of particles during radioactive decay: α-particles, comprised of two protons and two neutrons, are larger in size and exhibit limited penetration power with a radiation range of less than 100 μm; β-particles, which are high-speed electrons or positrons, possess stronger

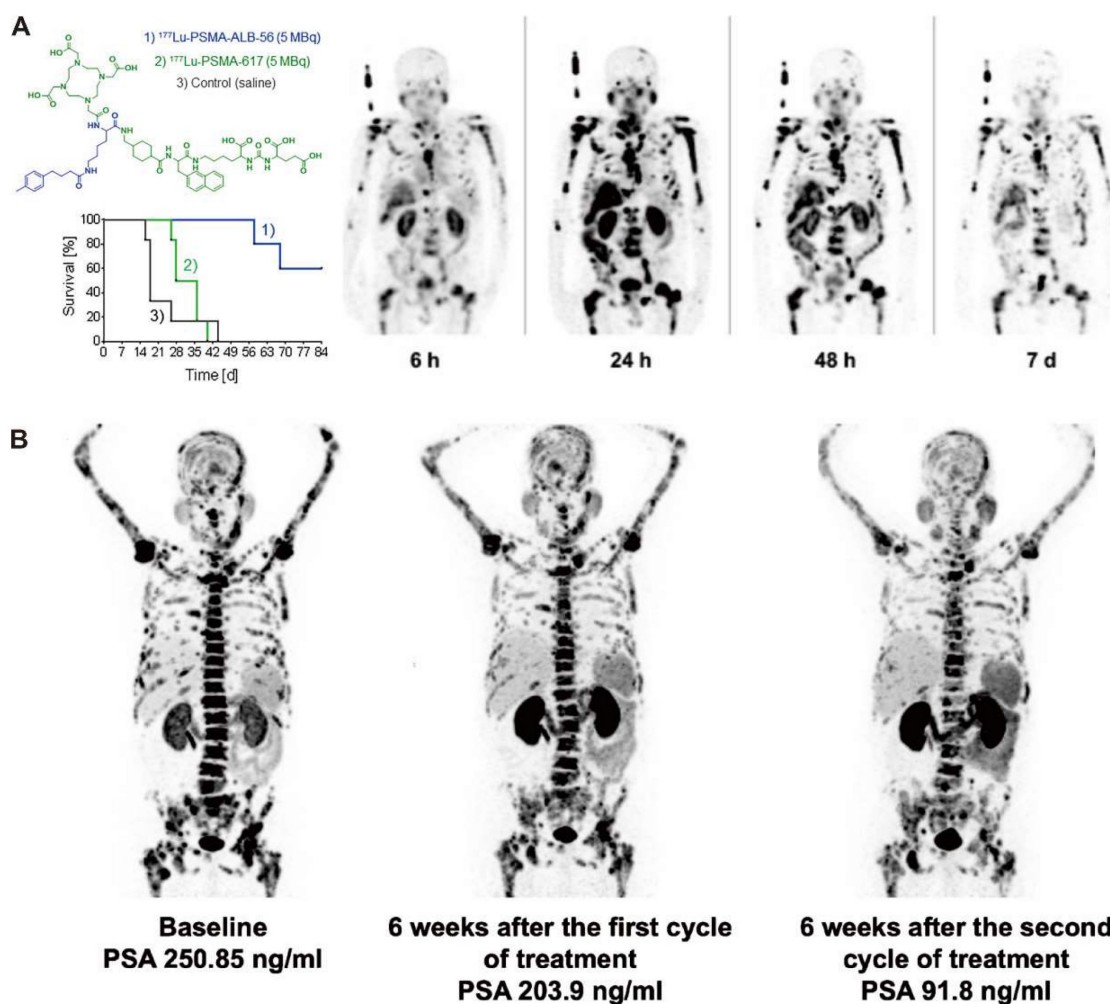


**Figure 4.** Clinical application of representative PSMA-617 albumin-binding derivatives. A. Preclinical survival impact in mice from [<sup>177</sup>Lu]Lu-PSMA-ALB-56 vs. [<sup>177</sup>Lu]Lu-PSMA-617 treatment (left) and clinical SPECT images of [<sup>177</sup>Lu]Lu-PSMA-ALB-56 (right). Adapted with permission from [66, 70], Copyright 2022 Society of Nuclear Medicine and Molecular Imaging and 2020 Springer Nature. B. Representative mCRPC patients for [<sup>68</sup>Ga]Ga-PSMA PET/CT and PSA response evaluation in the phase I trial to determine the maximum tolerated dose and patient-specific dosimetry of [<sup>177</sup>Lu]Lu-LNC1003. Adapted with permission from [72], Copyright 2022 Springer Nature.

penetration capabilities and can have a radiation range of up to 2 mm, and are therefore more likely to generate crossfire effects; Auger electrons, excited electrons released in the process of inner shell electron ionization or disassociation from the atomic nucleus, typically have a range from nanometers to micrometers, primarily exerting effects at a microscopic scale. Understanding these differences is crucial for assessing their biological effects and implementing appropriate radiation safety measures. Beyond the commonly utilized clinical radionuclides such as  $^{90}\text{Y}$ ,  $^{177}\text{Lu}$  and  $^{225}\text{Ac}$ , a new generation of radionuclides is gradually gaining attention. Terbium is interesting because it comprises four medically relevant radioisotopes, including terbium-149, terbium-152, terbium-155, and terbium-161. These radioisotopes share identical chemical characteristics, enabling the preparation of radiopharmaceuticals with identical pharmacokinetics. They can be employed for PET (terbium-152) and SPECT (terbium-155) imaging, as well as for  $\alpha$ - (terbium-149) and  $\beta$ -particle (terbium-161) therapy [74, 75]. Interestingly, terbium-161 has similar characteristics to  $^{177}\text{Lu}$  but co-emits a substantial number of conversion and Auger electrons. The first-in-human application of  $^{161}\text{Tb}$ Tb-DOTATOC demonstrated the feasibility of imaging even small metastases in a first-in-human application [76]. Recent phase I/II clinical trials are currently being conducted in mCRPC patients using  $^{161}\text{Tb}$ Tb-PSMA-I&T (NCT05521412),  $^{161}\text{Tb}$ Tb-DOTA-LM3 (NCT05359146) and  $^{161}\text{Tb}$ Tb-PSMA-617 (NCT05521412). Except  $^{225}\text{Ac}$ , other hopeful radionuclides for  $\alpha$ -therapy include terbium-149, astatine-211, bismuth-212, bismuth-213, lead-212, radium-223, and thorium-227 [77]. Terbium-149 decreases with a short half-life of only 4.1 h, making it suitable for small molecules with fast tumor accumulation and efficient clearance. It emits low-energy  $\alpha$ -particles without substantial numbers of  $\alpha$ -emitting daughter nuclides and its co-emission of  $\beta^+$ -particles, enabling PET imaging of  $^{149}\text{Tb}$ -labeled radioligands [78]. A preferred short decay chain minimizes daughter recoil toxicity, thereby reducing unnecessary radiation exposure and dose burden [79]. For  $^{225}\text{Ac}$ , effective imaging remains a challenge; to simulate the distribution of  $^{225}\text{Ac}$ -labeled tumor-targeting agents, lanthanum-132 may be used as an imaging surrogate with similar tumor uptake and biodistribution patterns [80].

## Nanotheranostics

### Advantages of nanotechnology

Nanotechnology has made it possible to combine

diverse therapeutic agents by physical adsorption or chemical binding, to obtain multifunctional nanomaterials for theranostics [81]. Nanomaterials have prominent advantages over small molecules in the following aspects: First, nanomaterials can passively accumulate and preferentially remain in the tumor by the enhanced permeability and retention effect [82]. Second, owing to the presence of diverse functional groups, the surface of nanomaterials can be easily modified with proteins, peptides, and other biomolecules, which enable targeted accumulation in the tumor tissue [83]. Third, benefiting from the high surface area to volume ratio of nanomaterials, high loading efficiency of therapeutic agents can be achieved, protecting them from enzymatic degradation [84]. Last but not least, the functionalized nanomaterials can control drug release via either internal or external stimuli, such as pH changes, increased glutathione levels and light impulses [85-87] to prevent unexpected drug leakage, and diminish or mitigate the potential side effects through exposure of the drug to healthy tissues.

Nanomedicine equipped with both therapeutics and diagnostics functionalities based on nanoparticle synthesis and engineering is referred to as nanotheranostics [84]. The field is associated with both basic science and clinical applications, especially cancer treatment. Recent progress in nanotheranostics has focused on the interaction between NPs and tumors, the creation of nanomedicines for personalized treatment and the prevention of tumor metastasis and recurrence [88]. These applications, however, require a general approach to solving clinical issues and improving treatment outcomes by intervening both diagnosis and therapy. In this part, we will summarize the recent progress of nanotheranostics, including photo- [87, 89-112], sono- [113-125], chemo- [126-137] and immuno-theranostics [138-146]. Further, the challenges of nanotheranostics will also be discussed.

### Phototheranostics

Phototherapy, consisting of photodynamic and photothermal therapy, can induce cell apoptosis by the photogeneration of reactive oxygen species (ROS), which has shown great potential for cancer treatment [147]. There are two general ways in the photosensitization process: one is the hydrogen/electron transfer (type I) for the generation of superoxide radical ( $\text{O}_2^{\cdot-}$ ) and hydroxyl radical ( $\text{OH}\cdot$ ), and the other one is the direct energy transfer (type II) for the generation of singlet oxygen ( $^1\text{O}_2$ ) [148, 149]. The phototherapeutic efficacy, however, is usually compromised by several factors, such as penetration depth and tumor hypoxia. To address these issues, significant efforts have been

devoted to enhancing the penetration depth, relieving tumor hypoxia, or developing hypoxia-tolerant therapies [149]. These therapies are often guided by fluorescence or photoacoustic imaging.

The second near-infrared (NIR) window (NIR-II, 1000-1700 nm) optical imaging is advantageous over NIR-I window due to its high signal-to-noise ratio, low autofluorescence, and high tissue penetration depth [150]. Inorganic NPs, especially lanthanide-based NPs, show large Stokes shift, sharp emission peaks, and type-determined emissions in a broad spectrum (1000-3000 nm), and are therefore ideal for

fluorescence imaging and sensing [151]. For example, Zhang *et al.* reported a series of lanthanide-doped NPs with an extended emission lifetime in the NIR-II window for resolving mouse abdominal vessels, tumors, and ureters in deep tissue (~2-4 mm) [92]. Such lifetime imaging approach benefits from higher signal-to-noise ratios as well as a threefold greater sharpness. They also reported a hybrid erbium(III)-bacteriochlorin probe, facilitating robust NIR imaging with high contrast and spatial resolution (Figure 5A) [93].

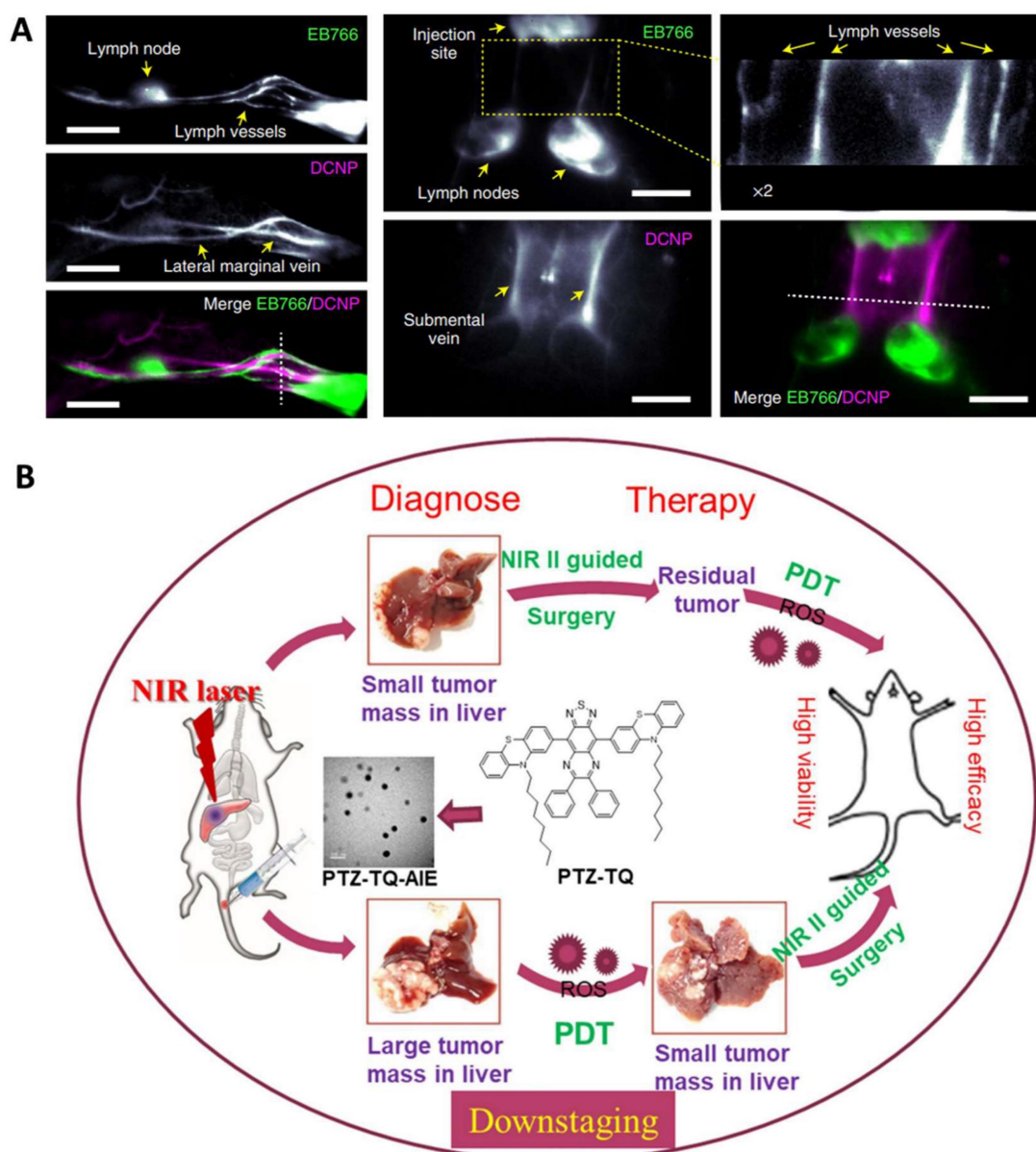


**Figure 5.** Representative nanomaterials for NIR-II imaging guided theranostics. A. Imaging of neck lymph and blood vessels with the molecular complex EB766 and downconversion NPs, cross-sectional intensity profile along the white dashed line. Mouse hindlimb lymph structures (EB766) and blood vessels (downconversion NPs) in different regions of a mouse and cross-sectional intensity profile along the white dashed line. Scale bars, 4 mm. Adapted with permission from [93], Copyright 2021 Springer Nature. B. Schematic illustration of NIR-II emissive AIEgen photosensitizer PTZ-TQ that enables ultrasensitive imaging-guided surgery and phototherapy to fully inhibit orthotopic hepatic tumors. Adapted with permission from [91], Copyright 2021 Springer Nature.

Apart from inorganic materials, organic photosensitizers, especially those with aggregation-induced emission (AIE), have great potential for phototheranostics in that they can overcome the barrier of aggregation caused fluorescence and ROS quenching [94, 152, 153]. For example, Chen *et al.* reported a photostable AIEgen dots (7,7'-(6,7-diphenyl-[1,2,5]thiadiazolo[3,4-g] quinoxaline-4,9-diyl)bis(10-octyl-10H-phenothiazine)) with NIR-II emission at 1250 nm which can be extended to 1600 nm (Figure 5B) [91]. Such dots efficiently generated ROS for PDT against orthotopic liver tumors both *in vitro* and *in vivo*. As a result, both image-guided surgery of early-stage tumors and inhibition of tumor recurrence can be achieved with minimal side effects.

Continuous irradiation during PDT can deteriorate tumor hypoxia because it not only consumes intracellular oxygen but also damages tumor blood vessels, limiting the phototherapeutic effect [90]. To improve PDT performance, there are generally two ways to relieve tumor hypoxia: one is the delivery of the molecular oxygen to the tumor using carriers, such as perfluorocarbon [87, 97, 102], and the other one is fractionated PDT [98, 101, 103]. *In situ* reversible capture and slow release of  $^1\text{O}_2$  are considered as an appropriate alternative to maintaining  $^1\text{O}_2$  generation under dark conditions. The photosensitization and chemical release of  $^1\text{O}_2$  overcomes PDT-induced hypoxia for improved efficacy. Inspired by these observations, Chen *et al.* reported two typical moieties (pyridione and anthracene) that can reversibly capture and release singlet oxygen in the TME, respectively (Figure 6A and 6B). The authors linked pyridione onto polyethylene glycol (PEG) to encapsulate a heavy atom-free photosensitizer 2,5-bis(2-ethylhexyl)-3,6-bis(5-(4-(1,2,2-triphenylvinyl)phenyl)furan-2-yl)-2,5-dihydropyrrolo[3,4-c]pyrrole-1,4-dione (DPPTPE) [112] or conjugated anthracene onto the BODIPY core to prepare 10-(anthracen-9-yl)-3,7-bis((E)-4-(diphenylamino)styryl)-5,5-difluoro-1,9-dimethyl-5H-dipyrrolo[1,2-c:2'',1'' f ][1,3,2] diazaborinin-4-ium-5-uide (ABDPTPA) [104]. The singlet oxygen half-life was prolonged, and the hypoxia was relieved, leading to an enhanced therapeutic efficacy, compared with non-fractionated delivery of singlet oxygen strategies. Compared with DPPTPE NPs, ABDPTPA NPs with NIR-II emission also allowed for low background imaging with a high signal-to-noise ratio.

Efficient hydrogen/electron transfer can contribute to the generation of superoxide or hydroxyl radicals, which are more cytotoxic than singlet oxygen [105-107, 109, 111, 154]. In addition, hydroxyl radicals originating from water or

intercellular hydrogen peroxide can overcome the oxygen dependence for hypoxia-tolerant type I PDT [154]. For example, Li *et al.* conjugated a 2,4,6-tris(N,N-dimethylaminomethyl)phenoxy group onto zinc(II) phthalocyanine (Pc) to prepare PcA, which can self-assemble to form NPs with a strong generation of superoxide radicals, providing a promising application in antibacterial treatment (Figure 7A) [110]. Another example by Tang *et al.* is the fabrication of precise nuclear targeting PDT protocol based on type-I photosensitizers with AIE characteristics [108]. 2-((5-(4-(phenyl(4-(1,2,2-triphenylvinyl)phenyl)amino)phenyl)furan-2-yl)methylene) malononitrile exhibits AIE property and stronger type-I ROS generation ability, owing to tetraphenylethylene conjugation induced smaller singlet-triplet energy gap (Figure 7B). With the aid of a lysosomal acid-activated trans-activator of transcription-peptide-modified amphiphilic polymer poly(lactic acid)<sub>12k</sub>-poly(ethylene glycol)<sub>5k</sub>-succinic anhydride-modified trans-activator of transcription, the corresponding TTFMN-loaded NPs accompanied with acid-triggered nuclear-targeting peculiarity, which can be visualized by fluorescence imaging, and can quickly accumulate in the tumor site and effectively suppress the tumor growth with the help of laser irradiation.

## Sonotheranostics

Like PDT, sonodynamic therapy (SDT) is a non-invasive therapeutic method that utilizes a sonosensitizer to generate ROS when triggered by ultrasound [155, 156]. It benefits from a deep penetration depth, allowing the treatment of lesions at varying depths by reducing cell viability, thereby preventing tumor recurrence [113-118]. Sonodynamic therapy induces cytotoxic effects only when stimulated by ultrasound externally in the cancerous region [119-124]. Without ultrasound, the drug is non-toxic. However, once the drug is exposed to ultrasound and molecular oxygen, ROS is generated to induce cell death. Ultrasound imaging is usually utilized to better understand the uptake of the nanomaterials, which can help determine an accurate time point for SDT. Recent sonotheranostics commonly focused on the design and preparation of novel sonosensitizers, or the combination of sonodynamic therapy with other therapeutic methods. Among the various sonosensitizers, metal organic frameworks [125, 157], covalent organic frameworks [114], and layered double hydroxide [122] have been widely employed, especially porphyrin derivatives [120]. In this part, the recent progress of sonodynamic therapy combined with

other therapeutic methods will be discussed.

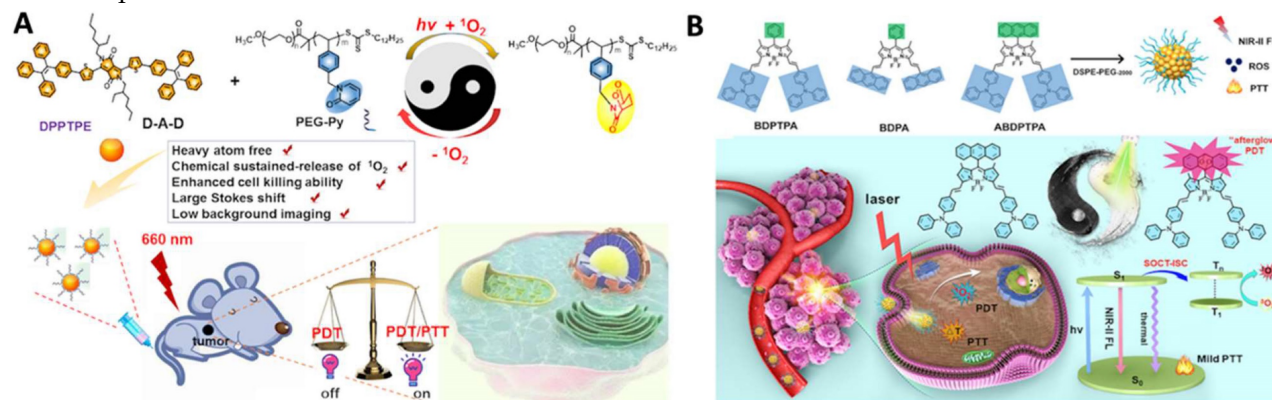


**Figure 6.** Representative work of fractionated delivery of singlet oxygen for cancer theranostics. A. Illustration of the nanoformulation structure. Adapted with permission from [112], Copyright 2020 Wiley-VCH. B. Anthracene functionalized photosensitizers for fractionated delivery of singlet oxygen with enhanced phototheranostics. Adapted with permission from [104], Copyright 2021 Wiley-VCH.

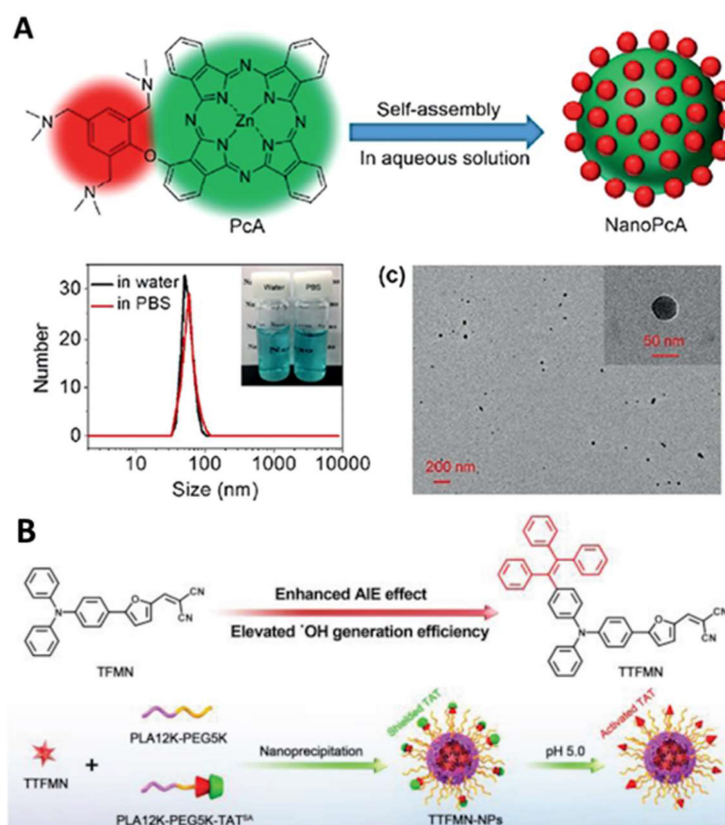


**Figure 7.** Typical examples of designing type I photosensitizers for cancer theranostics. A. Preparation and characterization of NanoPcA by TEM and DLS. Adapted with permission from [110], Copyright 2020 Wiley-VCH. B. Illustration of molecular design of TFMN and TTFMN, mechanisms of type-I and II processes, construction of acid-activated TTFMN NPs, and their applications in precise photodynamic nuclear targeting cancer therapy. Adapted with permission from [108], Copyright 2021 Wiley-VCH.

Carbon monoxide (CO) based gas therapy has attracted attention as an anti-tumor technique due to the CO release induced cytotoxicity [119]. Sono-dynamic-CO gas therapy may overcome the oxygen dependence for hypoxic tumor treatment. For example, Li *et al.* reported the synthesis of two rhenium(I) tricarbonyl complexes for ultrasound-triggered CO release and ROS generation [119]. Re-NMe<sub>2</sub> releases CO triggered by ultrasound and shows high cytotoxicity to tumor cells in vitro and in

vivo. The strong ROS generation as well as CO release makes it a promising tool for the treatment of hypoxic tumors.

SDT can also be used to activate an immune response, with programmed death-ligand 1 (PD-L1) being a promising immune checkpoint that can be targeted for cancer treatment [117]. Jiang *et al.* prepared a metal organic framework nano-catalyst consisting of porphyrin and dysprosium for SDT and reduction of PD-L1 expression (Figure 8A) [117]. The

CD47 overexpression and suppressive tumor-associated macrophages (TAMs) lead to treatment failure. Consequently, Gong *et al.* proposed a biomimetic nanodrug (abbreviated as MPIRx) by co-loading RRx-001 (a CD47 inhibitor) and IR780 (a sonosensitizer) into PEG-PCL nanomicelles, which were then coated with osteosarcoma cell membranes (Figure 8B) [116]. This nanoformulation significantly inhibited osteosarcoma proliferation and migration, inducing apoptosis and immunogenic cell death (ICD). Furthermore, MPIRx was able to promote M1-type polarization and increase the phagocytosis activity of macrophages.

Afterglow luminescence molecular imaging minimizes tissue autofluorescence and increases the signal-to-noise ratio [124]. The 'sonoafterglow', however, has been rarely reported. Recently, Xu *et al.* developed an organic NPs capable of producing ultrasound-induced afterglow for application in cancer immunotheranostics (Figure 9) [124]. Benefiting from being brighter and detectable in deep tissue (4 cm), such NPs comprising a sonosensitizer can subsequently activate a substrate for the emission of afterglow luminescence more efficiently than the traditionally reported light-induced afterglow. Systemic delivery of the NPs allowed for sonoafterglow-guided treatment of mice bearing subcutaneous breast cancer tumors. The molecular sonoafterglow imaging with high sensitivity and depth may offer a new paradigm for the monitoring of physiopathological processes.

Apart from basic science applications, SDT holds potential for clinical translation [158, 159]. For example, Zha *et al.* have initiated a phase I clinical trial SDT combined with temozolomide for the treatment of recurrent glioblastoma, a cancer with poor prognosis and ineffective treatments (Trial

information: Chinese Clinical Trial Registry (<http://www.chictr.org.cn/>): ChiCTR2200065992) [159]. None of the nine patients in this study suffered from any clinical, hematological, neurological, or skin-targeted adverse effects. After the completion of the trial, eight patients experienced disease progression, but one patient maintained stable disease. However, the number of patients in this study was small and a long-term survival benefit was not demonstrated. In a separate study, Syed *et al.* started both first in human phase I/II study with aminolevulinic acid for pediatric diffuse intrinsic pontine glioma SDT [158]. Preclinical results have shown that SDT through MR-guided focused ultrasound to activate protoporphyrin IX can slow the growth of gliomas and extend survival in animal models. Further, the patients tolerated the procedure well without any adverse effects. The first-in-human experience with a new therapeutic modality for diffuse intrinsic pontine glioma patients demonstrated that aminolevulinic acid SDT is safe at 200 J. Therefore, ascending drug and low-intensity focused ultrasound energy dose combinations should be further investigated to evaluate pharmacokinetics and radiographic evidence of tumor physiological changes.

## Chemotheranostics

Chemotherapy utilizes anti-cancer drugs, such as genotoxic or alkylating agents, as part of a standardized treatment regimen [130, 135]. Chemotherapy aims to prolong life with a curative intent by inhibiting mitosis or inducing DNA damage and it is one of the major categories of the medical discipline specifically dedicated to pharmacotherapy, known as medical oncology [155, 156].

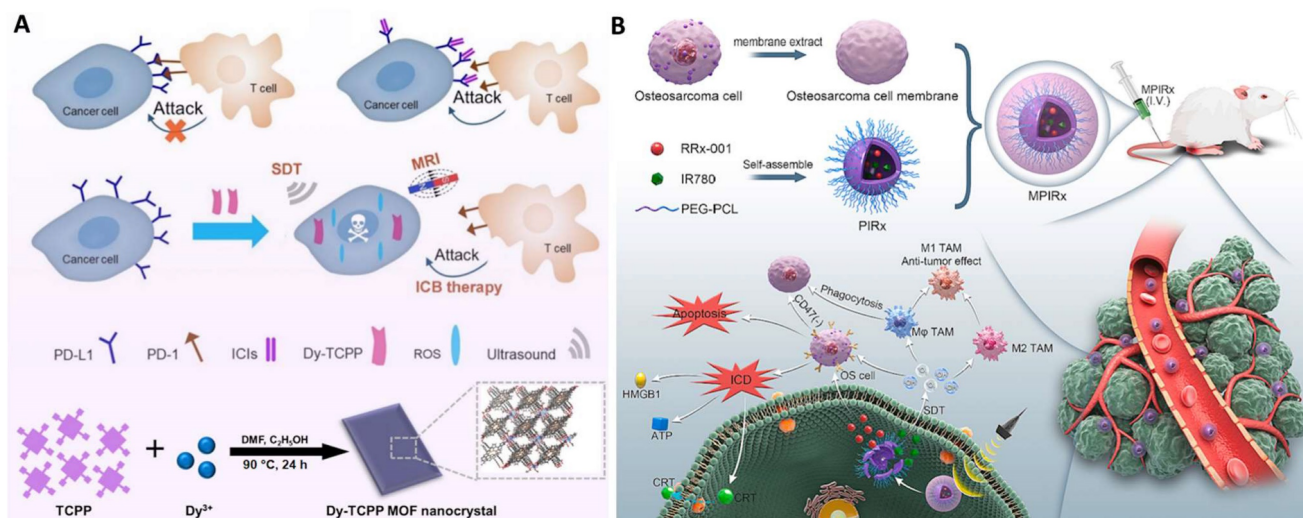


**Figure 8.** A. Representative nanomaterials for sonoatheranostics. Illustration of Dy-TCPP nanocrystals killing cancer cells by the combination treatment of SDT and immunotherapy. Adapted with permission from [117], Copyright 2023 Springer Nature publishing group. B. The preparation of MPIRx nanodrugs for SDT and CD47 inhibitors. Adapted with permission from [116], Copyright 2023 Elsevier publishing group.

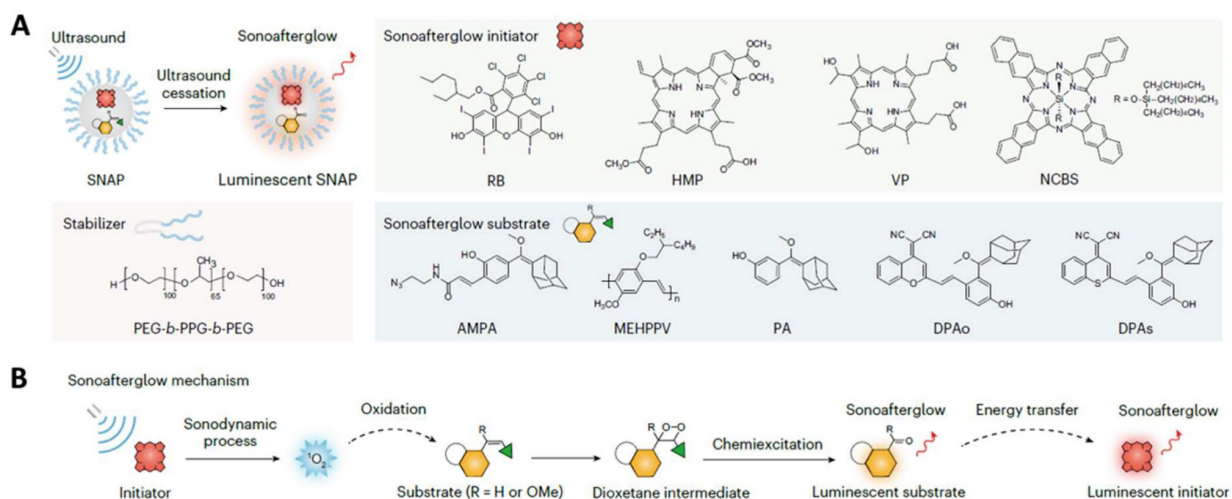


**Figure 9.** Representative work of sonoafterglow theranostics. A. Illustration of sonoafterglow initiators and substrates. B. Molecular mechanism of sonoafterglow. Initiators generate  $^1O_2$  to convert substrate into active dioxetane substrates under ultrasound application, emitting afterglow luminescence. The luminescence can transfer back to sonosensitizer and re-emit at longer wavelength. Reproduced from ref [124] with permission. Copyright 2023 Nature Publishing Group.

Traditional anti-cancer drugs usually suffer the fact that they are not targeted to the tumor tissue but, rather, affect all tissues in the body. Severe side effects frequently occur as a consequent damage to normal tissue. Nanomedicine may provide a much-needed boost by improving the potency of virtually any anti-cancer drug, mostly by optimizing bioavailability and tissue-specific deposition while limiting off-site effects [83, 88]. For example, Palange *et al.* designed a biodegradable hydrogel microparticle by cross-linking PEG with hydrolyzable 1,4-dithiothreitol, which had been loaded with 200 nm NPs carrying therapeutic and imaging agents (Figure 10A) [130]. Fluorescence imaging revealed that docetaxel-nanoparticles colocalized with pulmonary metastatic foci, prolonged the retention of chemodrug at the diseased site, suppressed lesion growth, and boosted survival beyond 20 weeks post nodule engraftment. Another example by Kumar *et al.* is the use of a lipid polymeric nanohybrid delivery system. They constructed a methotrexate-loaded nano lipid polymer system to controllably transport methotrexate in MCF-7 cells through endocytosis via phosphatidylcholine (Figure 10B) [127]. This kind of system prolonged the drug circulation time in the system and prevented drug discharge.

Synergistic combination therapies may have advantages over monotherapies. Chemotherapy has been combined with other therapeutic methods, such as phototherapy [126, 128, 129, 132, 136, 137, 160] and chemodynamic therapy (CDT) [131, 133, 134]. Since phototherapy has been discussed in the previous section, CDT will be exemplified to demonstrate the

power of combination therapies with synergistic effects. As an exceptionally discerning and internally triggered therapeutic approach, CDT has demonstrated significant promise for the targeting of tumors while reducing systemic side effects [134]. Transition metal-based nanomaterials, especially Cu(II) and Fe(II), can initiate the Fenton or Fenton-like reaction to catalyze hydrogen peroxide ( $H_2O_2$ ) to generate cytotoxic hydroxyl radicals ( $OH\cdot$ ) even under the hypoxic TME, leading to cell apoptosis. For example, Yang *et al.* synthesized artesunate-loaded polydopamine/iron nanocomplexes and then coated them with fibronectin (FN). Improved CDT effectiveness was attained through the simultaneous administration of  $Fe^{2+}$  and artesunate, as they synergistically enhanced intracellular ROS production. This enhancement arose from a cyclic reaction involving the conversion of  $Fe^{3+}$  to  $Fe^{2+}$  via  $Fe^{3+}$ -mediated glutathione oxidation and the reduction of artesunate mediated by  $Fe^{2+}$  in the Fenton reaction (Figure 11A) [133]. Guided by MRI, this synergistic therapy induced noticeable ICD in combination with antibody-mediated immune checkpoint blockade, resulting in significant anti-tumor immunity.

Trimodal therapy may further enhance therapeutic efficacy. Shi *et al.* designed an intelligent dual-responsive nanostructure for MRI-guided synergistic chemo-photothermal therapy-CDT (Figure 11B) [131]. Polydopamine,  $MnO_2$ , and hyaluronic acid were co-loaded into the drug-loaded hollow mesoporous silica NPs, which were responsive to both endogenous and external environments. On the

one hand, polydopamine provided pH responsiveness and photothermal conversion for drug delivery regulation and local hyperthermia, while  $\text{MnO}_2$  not only offered controlled drug release and enhanced CDT through glutathione depletion in the TME but also provided nano-enzyme properties for MR imaging by releasing  $\text{Mn}^{2+}$ . Chemo-photothermal therapy-CDT can eradicate tumors in less than two weeks.

## Immunotheranostics

Immunotherapy modulates the immune system for the treatment of diseases [161]. Activation immunotherapies aim to trigger or enhance an immune response, whereas suppression immunotherapies are intended to decrease or inhibit immune responses [162, 163]. A vaccine can provide active acquired immunity to a specific infectious or

malignant disease [141]. Through the activation of the body's immune system, the vaccine identifies the threat, eliminates it, and subsequently recognizes and eliminates any future encounters with microorganisms linked to that threat [163]. Despite the great advances in the field of vaccination, the development of novel and effective vaccines is still far from satisfactory [140]. Moreover, several existing vaccines occasionally encounter challenges such as incomplete immune system activation, *in vivo* instability, elevated toxicity, the necessity for a cold chain, and multiple administrations. Nanotechnology has emerged as a possible solution to address these issues. Essentially, nanovaccines represent a novel category of vaccines that utilize NPs as carriers and/or adjuvants. Capitalizing on the similar size of NPs to pathogens, this approach enables efficient immune system stimulation and the elicitation of robust cellular and

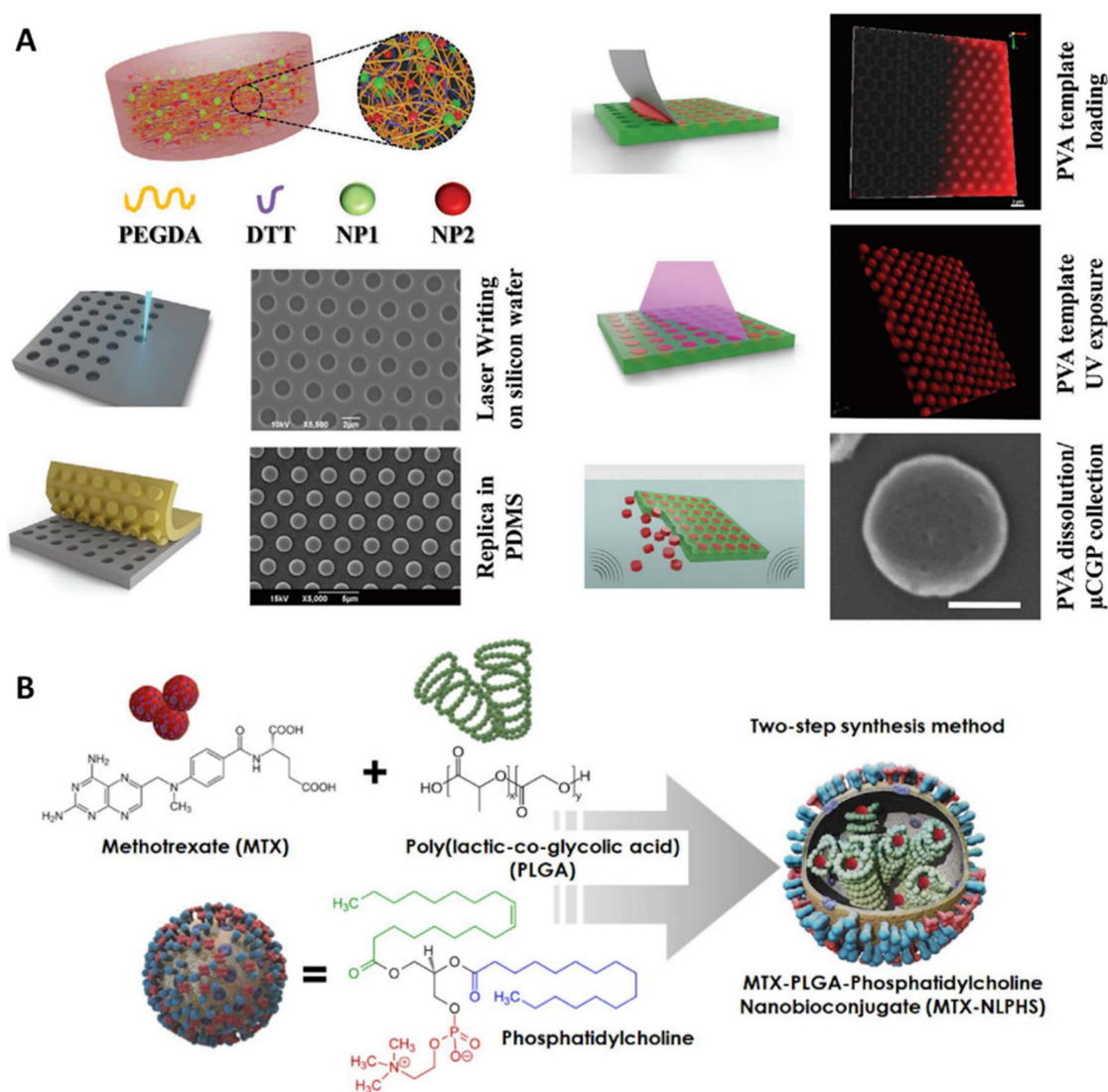


**Figure 10.** Representative work of nanomaterials for chemotheranostics. A. Synthesis and characterization of a spongy  $\mu$ CGP comprising multiple small NPs (nanoconstructs) dispersed within a porous PEG matrix. Adapted with permission from [130], Copyright 2023 Wiley-VCH. B. Schematic representation of nanohybrid MTX-NLPHS system formulation and its cellular internalization. Adapted with permission from [127], Copyright 2023 Ivyspring International Publisher.

humoral immune responses [140]. In this part, we will focus on the development of nanovaccine as immunotheranostics.

As mentioned above, ICD can be activated by external-beam radiotherapy, internal radiation therapy, chemotherapy, or PDT [143]. ICD can induce damage-associated molecular patterns released from dying tumor cells, thus eliciting an antitumor immune response [139] and is dependent upon the endoplasmic reticulum (ER) stress [164]. However, the short half-span of ROS and intracellular diffusion depth impair ER localization, limiting ER stress induction. Therefore, designing nanomedicine with ER targeting ability is a wise strategy to induce ER stress [164]. Inspired by these observations, Deng *et al.* designed and synthesized a PEG-s-s-1,2-distearoyl-sn-glycero-3-phosphoethanolamine-N-[amino-(polyethylene glycol)<sub>2000</sub>] NPs loaded with an ER-targeting photosensitizer 4,4',4'',4'''-(porphyrin-5,10,15,20-tetrayl)tetrakis(N-(2-((4-methylphenyl)sulfonamido)ethyl)benzamide) [139]. Fluorescence imaging was used to determine NP uptake and the optimum time point for laser therapy. Such NPs showed selective ER accumulation ability and strong ROS generation with NIR laser irradiation. As a result, ER stress was induced, ICD was amplified, and immune cells were activated, leading to augmented immunotherapeutic efficacy.

Cell-based immunotherapies are promising agents for cancer treatment [138, 142, 144, 146]. Immune effector cells, such as lymphocytes, dendritic cells (DC), macrophages, natural killer cells, and cytotoxic T lymphocytes cooperate to defend the body against cancer by targeting abnormal antigens that are expressed on the surface of tumor cells. Apart from DC cell membranes, macrophages based nano-

vaccines have also emerged as an encouraging therapeutic strategy [145]. However, activating macrophages for antitumor immunotherapy is faced with two major challenges. Known as a “don't eat me” signal on cancer cells, ligation of signal regulatory protein alpha (SIRP $\alpha$ ) on macrophages to CD47 prevents macrophage phagocytosis of cancer cells. Additionally, colony-stimulating factors polarize TAMs to a tumorigenic M2 phenotype [145]. Encouraged by these observations, Rao *et al.* genetically engineered cell-membrane-coated magnetic NPs (gCM-MNs) to efficiently block the CD47-SIRP $\alpha$  pathway and simultaneously include an MN core to promote M2 TAM repolarization [145]. Moreover, the gCM shell protected the MNs to escape immune clearance; and in turn, the MN core delivered the gCMs into tumor tissues under magnetic navigation to promote systemic circulation and tumor accumulation. gCM-MNs significantly prolonged overall mouse survival by controlling both local tumor growth and distant tumor metastasis in melanoma and breast cancer models. To extend this work, the authors have also constructed hybrid cell membrane nanovesicles (denoted as hNVs) containing SIRP $\alpha$  variants with significantly increased affinity to CD47 [144]. The hNVs can block the CD47-SIRP $\alpha$  signaling axis as well as promote M2-to-M1 repolarization within the TME. Similarly, both local recurrence and distant metastasis have been prevented in malignant melanoma models.

T-cells play a pivotal role in modulating the immune response and assessing the prognosis of cancer treatments that rely on immune activation. While specific biomarkers determine the T cell population and distribution within tumors, the *in situ* activity of T cells has been rarely reported. To address

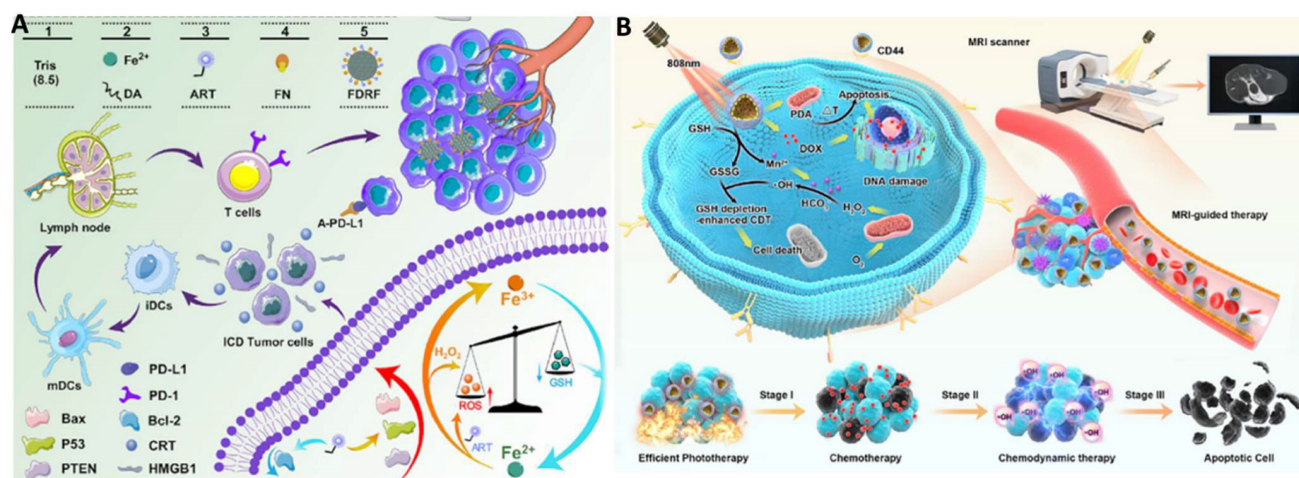


**Figure 11.** Representative work of nanomaterials for chemo-CDT. A. Microfluidic synthesis of FDRF NCs for T1-MRI guided chemo-CDT of tumors. Adapted with permission from [133], Copyright 2023 Elsevier Publishing Group. B. Schematic illustration of TME-responsive HSPMH-DOX for activation MRI guided synergistic therapy. Adapted with permission from [131], Copyright 2023 Elsevier Publishing Group.

this issue, Zhou *et al.* developed fusogenic liposomes to regulate and measure T cell activity by targeting their surface redox status as a chemical marker [165]. These T cell-targeting fusogenic liposomes, equipped with 2,2,6,6-tetramethylpiperidine groups, neutralize reactive oxygen species, safeguarding T cells from oxidative damage that could impair their activity. Simultaneously, the generation of paramagnetic 2,2,6,6-tetramethylpiperidine 1-oxyl radicals enabled magnetic resonance imaging to quantify T-cell activity. This enabled the dynamic visualization of T-cell activity. In various mouse models, these T-cell-targeting fusogenic liposomes demonstrated effective tumor suppression and early prediction of radiotherapy outcomes.

Nanomedicines co-delivering DNA, RNA, and peptide therapeutics are highly desirable but underdeveloped tools for cancer theranostics [166]. In one example, Zhu *et al.* reported self-assembled intertwining DNA-RNA nanocapsules (iDR-NCs) for the efficient delivery of synergistic DNA CpG, short hairpin RNA (shRNA) adjuvants, and tumor-specific peptide neoantigens into antigen-presenting cells present in lymph nodes [166]. The uptake of the NPs was imaged by PET. CpG and shRNA in iDR-NCs activated APCs for sustained antigen presentation. Notably, iDR-NC/neoantigen nanovaccines resulted in an 8-fold increase in neoantigen-specific peripheral CD8<sup>+</sup> T-cells compared to CpG, activated T cell memory, and significantly led to the regression of neoantigen-specific colorectal tumors.

### Challenges of nanotheranostics

Although different NPs have been reported as potential cancer therapeutics, only a handful have been approved by the FDA [88]. The disconnection between clinical translation and academic output in the field of nanomedicine is disheartening. This disparity may be attributed to several factors. Firstly, nanomedicines face various challenges, including unclear toxicities, issues with reproducibility, and the high cost of manufacturing NPs. The composition, assembly method, surface properties, rigidity, and charge all influence the structure of NPs, complicating the assessment of their potential toxicity. Secondly, the pursuit of reproducibility imposes limitations on the scale-up of NPs, as synthesizing NPs with specific properties in a rapid, precise, and consistent manner can be challenging. Thirdly, unlike biologics and small molecules that adhere to predetermined standards, nanomedicines are subject to complex chemistry, manufacturing, and control requirements, which necessitate adherence to various but interconnected regulations. Consequently, NPs often prove to be economically burdensome due to labor

and material costs.

Limitations exist in employing imaging to enhance nanotherapies. These encompass difficulties in attaining adequate spatial and temporal resolution for precise visualization of nanoparticles within intricate biological contexts. Concerns also arise regarding the potential interference of imaging agents with the therapeutic functionalities of nanoparticles. Moreover, the high expense and restricted availability of certain imaging modalities could impede their broad application in clinical settings. Nonetheless, continual advancements in imaging technology and nanoparticle design offer hope for surmounting these challenges and augmenting the effectiveness and safety of nanotherapeutic interventions.

### New horizons in theranostics: using synthetic biology

In addition to the well-known domains of nano- and radiotheranostics, researchers are exploring new ways to combine diagnostics with precision therapy. One such approach is to re-engineer the cells themselves; known as synthetic biology. Synthetic biology is a growing and inherently multidisciplinary field of science found at the crossroads between molecular biology, engineering, physics, and computational sciences [167, 168]. At its core, synthetic biology seeks to utilize molecular biology tools and techniques along with engineering approaches to design novel biological components and systems, or to repurpose existing biological components for useful purposes. This approach allows the creation of artificial cellular networks that are not naturally present in organisms and can be used to alter cellular behavior. The understanding and ability to modify biological tools have been largely made possible thanks to technological advances in genetic engineering and molecular biology. The first breakthrough was the development of cloning, a process by which genes can be transferred between organisms [169]. In conjunction with cloning techniques, DNA synthesis technologies have accelerated the rate at which synthetic constructs can be made [167]. Furthermore, advances in computational tools for DNA sequencing provided researchers with extensive databases of biological components, their functions, and interactions. These discoveries thus enabled an approach to create artificial networks by drawing upon an ever-expanding list of existing biological tools (or “*bio-tools*”). *Bio-tools* are likely to be proteins, enzymes, transcription factors and promoters (DNA elements that regulate gene expression). Such *bio-tools* can also be reporter genes or therapeutic genes. Therefore, harnessing the power of molecular

imaging can be beneficial for identifying and developing new therapeutic, diagnostic or theranostic avenues [170]. The *bio-tools* that are generated by DNA technologies can be improved and optimized by molecular evolution and computational modeling. They can also be assembled into gene circuits, that have an input such as, chemical compounds, metabolites, drugs, light or electromagnetic radiation and the output could be light, metabolites, therapeutic molecules, radiofrequency etc. As a result, gene circuits can potentially tie the expression of therapeutic or imaging agents to specific external stimuli or biological processes. This can improve the spatial and temporal precession of the treatment and consequently reduce side effects.

Several genes have been suggested as theranostic genes. In this case, the requirement should be that the gene – which usually encodes an enzyme – will not have a human homolog or, at least, have a specific substrate that is not catalyzed by the human homolog. The substrate should be converted from a non-reactive pro-drug to an active drug, usually with a cytotoxic effect. The same enzyme could convert an additional substrate to an imaging readout, i.e., a substrate detected by a noninvasive imaging modality. One example of this theranostic approach is the enzyme cytosine deaminase. In nature, cytosine deaminase is expressed either by bacteria or yeast. In both cases it converts cytosine to uracil by cleavage of an amine group. It can also convert the prodrug 5-fluorocytosine into a cytotoxic drug 5-fluorouracil [171]. While the prodrug or imaging agent can be delivered systemically, the gene can also be delivered using genetically manipulated migratory cells such as neural stem cells to the tumor site [172]. An elegant way to image the theranostic enzyme activity is using chemical exchange saturation transfer magnetic resonance imaging that can monitor the conversion of cytosine to uracil by removal of amine group with an exchangeable proton [173].

While synthetic biology allows the expansion of the toolbox for theranostics, it also poses some open questions and challenges for the bioengineering of next-generation synthetic *bio-tools* and circuits for theranostic purposes, as described in Table 2. To understand these challenges, we first must understand the available tools and how they can be used. Protein engineering is the process of modifying the amino acid structure of existing proteins, to create new proteins with new or improved properties [174, 175]. Approaches for protein engineering can be divided into two main categories: rational design and directed evolution. Rational design approaches depend on utilizing a deep understanding of a protein's structure and function to alter its structure

[174], whereas directed evolution techniques usually involve the use of random mutagenesis and screening criteria to find mutants with the desired properties [176]. Recent advances in computational modeling methods have been of great importance to protein engineering. Based on homology modeling and molecular dynamics, protein structure prediction tools like RoseTTA fold [177] and AlphaFold [178] are now able to make highly accurate structure predictions of proteins that still lack a crystal structure. By using such technology, proteins can be engineered to chelate different elements for diagnostic and therapeutic purposes. For example, recently the calcium sensor GCaMP, was modified to bind lanthanides [179]. This recombinant protein has an altered conformation and consequently is fluorescent. Moreover, binding of gadolinium to the protein termed Green Lanmodulin-based Reporter shortens the T1 relaxation of the surrounding water and thus can be used as an MRI contrast agent. Since the protein binds both light and heavy lanthanides, it has the potential to bind lutetium-177 and serve as a theranostic agent.

**Table 2.** Open questions and challenges in synthetic biology

Challenge	Proposed solution
How to develop a bio-tool that will not have crosstalk with the cell signaling machinery?	Using signaling pathways adopted from other organisms that use unorthodox cellular messengers.
How to allow remote activation of bio-tool?	Using light (optogenetics), chemicals (chemogenetics) or electromagnetic fields (magnetogenetics).
How to minimize the molecular or metabolic burden on the cells producing the bio-tools?	Using metabolic engineering, protein engineering, change the amino acid composition, optimize the DNA sequence.
How to deliver the gene circuits to the target tissue?	Developing the next generation of viruses, immune cells, stem cells, bacteria, and engineered microbiome.

In the last few decades, it has been shown that several proteins can be split into non-functional fragments that can spontaneously reassemble into a functional unit. The first example of this phenomenon can be traced back to ribonuclease S. It was shown that cleaving the enzyme at a single site produced individual fragments with decreased enzymatic activity but that these fragments had high affinity for each other and could interact to restore the original activity [180]. Split protein technology holds great promise for theranostics because it increases the precision of the treatment. Since a split protein can be activated on demand in specific locations, either by specific conditions or stimulus, or remotely (Table 2). This property offers the potential advantage of reducing background for imaging or side effects for treatment by minimizing off-target activation of proteins in surrounding tissues. Some prominent examples of split proteins include a split NanoBit®

that can be used in a single genetically encoded calcium sensor [181]. Recently, split NanoLuc was used to create a sensor for the neurotransmitter glutamate. Upon binding of glutamate, a marked increase in luminescence was observed [182, 183]. Bioluminescence has the potential to non-invasively stimulate nearby optogenetics for therapeutic purposes. Also noteworthy is the development of a split version of the sr39 mutant of HSV1-TK that was developed to study protein-protein interaction *in vivo* using PET [184], which also holds significant potential for use in gene therapy due to its “suicide” effect on tumor cells when present alongside the prodrug ganciclovir.

There are many ways to activate split enzymes, but perhaps one that is highly relevant for theranostic applications is magneto genetics, which utilizes magnetoreceptive molecules as a means of controlling the reconstitution of split proteins. Magnetoreception refers to the ability of certain organisms to perceive Earth’s magnetic field and it is a property that has been documented in many organisms, ranging from fish and birds to bacteria [185, 186]. The electromagnetic perceptive gene (EPG) [187] is a gene found in the glass catfish, *Kryptopterus vitreolus*, a fish known to respond to magnetic fields. When expressed in mammalian cells, EPG causes an increase in intracellular calcium in response to magnetic stimulation [187, 188]. Recently, EPG has been used in an adaptation of the split protein method, this approach utilizes a magnetic perceptive protein, as a “biomagnetic switch” that is controlled remotely by a magnetic field to drive the reconstitution of a split enzyme. Magnetogenetics has been deployed to activate enzymes in *E. coli* and mammalian cells. Notable examples of this technology include the creation of a split NanoLuc, a split Peroxidase and a split version of the theranostic gene HSV1-TK [189]. Upon stimulation with an electromagnetic field, it was demonstrated that the EPG split HSV1-TK can kill 4T1-Luc2 cancer cells in culture in the presence of the prodrug ganciclovir. While this technology is only in its infancy, it holds tremendous potential; both due to the therapeutic importance of HSV1-TK using pro-drugs such as ganciclovir and acyclovir, as well as its diagnostic importance for both PET [190] and MRI [191]. Improving imaging probes [192] or enzymes using protein engineering [193] technologies may lead in the future to more robust theranostic proteins.

The practicality and clinical translatability of synthetic biology are steadily increasing due to advancements in technology and research. In healthcare, synthetic biology has led to the development of novel therapeutics, such as engineered microbes for drug delivery and gene

editing tools for precise manipulation of genetic material. Additionally, synthetic biology enables the production of biomolecules like insulin and antibodies, which are crucial for treating various diseases. However, challenges remain, including standardization, scalability, safety, and ethical considerations [194]. Addressing these challenges is crucial for the widespread adoption of synthetic biology in clinical settings. Nonetheless, ongoing research and development efforts continue to improve the practicality and clinical translatability of synthetic biology, with promising prospects for revolutionizing medicine and biotechnology.

## Perspectives

In the past decade, the field of theranostics has undergone significant evolution, particularly in oncology. Here, we have dissected these advancements, with a focus on radiotheranostics and nanotheranostics. The concept of radiotheranostics has been increasingly adopted as a therapeutic strategy, demonstrating efficacy in the clinical treatment of thyroid cancer, NENs, and prostate cancer. Meanwhile, various strategies of nanotheranostics, including photo-, sono-, chemo-, and immuno-theranostics, each offer unique therapeutic strategies. However, it is currently premature to assert that theranostics is a sure cure for cancer. The field still faces basic challenges, such as improving targeting efficiency, reducing systemic toxicity, and addressing the heterogeneity of tumor response. Future research must also focus on overcoming the limitations in deep tissue penetration of therapeutic agents and enhancing the precision of diagnostic imaging. Moreover, additional clinical trials are needed to provide evidence that addresses key issues such as optimal treatment timing, dosing strategies, and management of complications. The development and clinical translation of theranostics is constrained by factors such as cost-effective production, scalability, and navigating regulatory landscapes.

The ongoing development of new theranostics approaches in academia and industry showcases the field's commitment to pioneering new research methods. Novel therapeutic targets and ligands in-turn will facilitate the development of new diagnostic agents. Theranostics continues to expand its boundaries through active research, aiming to transcend its current uses. Additionally, the concept of theranostics should be widened to include other combinations of imaging and therapy, as we have exemplified here with synthetic biology applications. While theranostics may not guarantee a cure for cancer, significant progress and continuous advancements emphasize its potential to improve

patient outcomes and revolutionize cancer treatment.

## Abbreviations

NPs: nanoparticles; FDA: Food and Drug Administration; NENs: neuroendocrine neoplasms; PET: positron emission tomography; SSTRs: somatostatin receptors; CT: computer tomography; PFS: progression-free survival; PSMA: prostate-specific membrane antigen; PI3K: phosphoinositide 3-kinase; PSA: prostate-specific antigen; mCRPC: metastatic castration-resistant prostate cancer; MRI: magnetic resonance imaging; rhPSMAs: radiohybrid PSMA inhibitors; CXCR4: C-X-C-motif chemokine receptor 4; FAP: Fibroblast activation protein; FAPI: FAP inhibitor; EB: Evans Blue; ROS: reactive oxygen species; NIR: near-infrared; AIE: aggregation induced emission; PDT: photodynamic therapy; TME: tumor microenvironment; PEG: polyethylene glycol; Pc: phthalocyanine; SDT: sonodynamic therapy; CO: Carbon monoxide; TAMs: tumor associated macrophages; ICD: immunogenic cell death; CDT: chemodynamic therapy; H<sub>2</sub>O<sub>2</sub>: hydrogen peroxide; FN: fibronectin; ER: endoplasmic reticulum; DC: dendritic cells; ASPIRE: antigen self-presentation with immunosuppression reversal; SIRPα: signal regulatory protein alpha; gCM-MNs: genetically engineered cell-membrane-coated magnetic NPs; hNVs: hybrid cell membrane nanovesicles.

## Acknowledgments

This work was supported by the National University of Singapore (NUHSRO/2020/133/Startup/08, NUHSRO/2023/008/NUSMed/TCE/LOA, NUHSRO/2021/034/TRP/09/Nanomedicine), National Medical Research Council (MOH-001388-00, MOH-001041, CG21APR1005, MOH-001127-00), Singapore Ministry of Education (MOE-000387-00), a Wellcome Trust Senior Research Fellowship (220221/Z/20/Z) and National Research Foundation (NRF-000352-00). This article is supported by the European Society for Molecular Imaging (ESMI). A dedicated “Theranostics a sure Cure for Cancer after 100 Years?” symposium was held at the 18th European Molecular Imaging Meeting (EMIM) where the idea for this review article was inspired (<https://e-smi.eu/>).

## Competing Interests

The authors have declared that no competing interest exists.

## References

- Pene F, Courtine E, Cariou A, Mira JP. Toward theragnostics. *Crit Care Med*. 2009; 37: S50-8.
- Weber WA, Barthel H, Bengel F, Eiber M, Herrmann K, Schäfers M. What Is Theragnostics? *J Nucl Med*. 2023; 64: 669-70.
- Seidlin SM, Marinelli LD, Oshry E. Radioactive iodine therapy; effect on functioning metastases of adenocarcinoma of the thyroid. *J Am Med Assoc*. 1946; 132: 838-47.
- Hertz S, Roberts A. Radioactive iodine in the study of thyroid physiology; the use of radioactive iodine therapy in hyperthyroidism. *J Am Med Assoc*. 1946; 131: 81-6.
- Solnes LB, Werner RA, Jones KM, Sadaghiani MS, Bailey CR, Lapa C, et al. Theragnostics: Leveraging Molecular Imaging and Therapy to Impact Patient Management and Secure the Future of Nuclear Medicine. *J Nucl Med*. 2020; 61: 311-8.
- Bodei L, Herrmann K, Schöder H, Scott AM, Lewis JS. Radiotheragnostics in oncology: current challenges and emerging opportunities. *Nat Rev Clin Oncol*. 2022; 19: 534-50.
- Adnan A, Basu S. Somatostatin Receptor Targeted PET-CT and Its Role in the Management and Theragnostics of Gastroenteropancreatic Neuroendocrine Neoplasms. *Diagnostics (Basel)*. 2023; 13.
- Strosberg J, El-Haddad G, Wolin E, Hendifar A, Yao J, Chasen B, et al. Phase 3 Trial of <sup>177</sup>Lu-Dotatate for Midgut Neuroendocrine Tumors. *N Engl J Med*. 2017; 376: 125-35.
- Sundlöv A, Gleisner KS, Tennvall J, Ljungberg M, Warfvinge CF, Holgersson K, et al. Phase II trial demonstrates the efficacy and safety of individualized, dosimetry-based <sup>177</sup>Lu-DOTATATE treatment of NET patients. *Eur J Nucl Med Mol Imaging*. 2022; 49: 3830-40.
- Hicks RJ, Kwakkeboom DJ, Krenning E, Bodei L, Grozinsky-Glasberg S, Arnold R, et al. ENETS Consensus Guidelines for the Standards of Care in Neuroendocrine Neoplasia: Peptide Receptor Radionuclide Therapy with Radiolabeled Somatostatin Analogues. *Neuroendocrinology*. 2017; 105: 295-309.
- Ginj M, Zhang H, Waser B, Cascato R, Wild D, Wang X, et al. Radiolabeled somatostatin receptor antagonists are preferable to agonists for *in vivo* peptide receptor targeting of tumors. *Proc Natl Acad Sci U S A*. 2006; 103: 16436-41.
- Wild D, Fani M, Behe M, Brink I, Rivier JEF, Reubi JC, et al. First Clinical Evidence That Imaging with Somatostatin Receptor Antagonists Is Feasible. *J Nucl Med*. 2011; 52: 1412-7.
- Krebs S, Pandit-Taskar N, Reidy D, Beattie BJ, Lyashchenko SK, Lewis JS, et al. Biodistribution and radiation dose estimates for <sup>68</sup>Ga-DOTA-JR11 in patients with metastatic neuroendocrine tumors. *Eur J Nucl Med Mol Imaging*. 2019; 46: 677-85.
- Cascato R, Waser B, Fani M, Reubi JC. Evaluation of <sup>177</sup>Lu-DOTA-sst2 antagonist versus <sup>177</sup>Lu-DOTA-sst2 agonist binding in human cancers *in vitro*. *J Nucl Med*. 2011; 52: 1886-90.
- Wild D, Fani M, Fischer R, Del Pozzo L, Kaul F, Krebs S, et al. Comparison of somatostatin receptor agonist and antagonist for peptide receptor radionuclide therapy: a pilot study. *J Nucl Med*. 2014; 55: 1248-52.
- Reidy-Lagunes D, Pandit-Taskar N, O'Donoghue JA, Krebs S, Staton KD, Lyashchenko SK, et al. Phase I Trial of Well-Differentiated Neuroendocrine Tumors (NETs) with Radiolabeled Somatostatin Antagonist <sup>177</sup>Lu-Satoreotide Tetraxetan. *Clin Cancer Res*. 2019; 25: 6939-47.
- Kaittani C, Andreou C, Hieronymus H, Mao N, Foss CA, Eiber M, et al. Prostate-specific membrane antigen cleavage of vitamin B9 stimulates oncogenic signaling through metabotropic glutamate receptors. *J Exp Med*. 2018; 215: 159-75.
- Nguyen T, Kirsch BJ, Asaka R, Nabi K, Quinones A, Tan J, et al. Uncovering the Role of N-Acetyl-Aspartyl-Glutamate as a Glutamate Reservoir in Cancer. *Cell Rep*. 2019; 27: 491-501.e6.
- Eder M, Schäfer M, Bauder-Wüst U, Hull WE, Wängler C, Mier W, et al. <sup>68</sup>Ga-complex lipophilicity and the targeting property of a urea-based PSMA inhibitor for PET imaging. *Bioconjug Chem*. 2012; 23: 688-97.
- Cho SY, Gage KL, Mease RC, Senthimithchelvan S, Holt DP, Jeffrey-Kwanisai A, et al. Biodistribution, Tumor Detection, and Radiation Dosimetry of <sup>18</sup>F-DCFBC, a Low-Molecular-Weight Inhibitor of Prostate-Specific Membrane Antigen, in Patients with Metastatic Prostate Cancer. *J Nucl Med*. 2012; 53: 1883-91.
- Afshar-Oromieh A, Malcher A, Eder M, Eisenhut M, Linhart HG, Hadaschik BA, et al. PET imaging with a [<sup>68</sup>Ga]gallium-labeled PSMA ligand for the diagnosis of prostate cancer: biodistribution in humans and first evaluation of tumour lesions. *Eur J Nucl Med Mol Imaging*. 2013; 40: 486-95.
- Zechmann CM, Afshar-Oromieh A, Armor T, Stubbs JB, Mier W, Hadaschik B, et al. Radiation dosimetry and first therapy results with a <sup>125</sup>I/<sup>131</sup>I-labeled small molecule (MIP-1095) targeting PSMA for prostate cancer therapy. *Eur J Nucl Med Mol Imaging*. 2014; 41: 1280-92.
- Heck MM, Tauber R, Schwaiger S, Retz M, D'Alessandria C, Maurer T, et al. Treatment Outcome, Toxicity, and Predictive Factors for Radioligand Therapy with (<sup>177</sup>)Lu-PSMA-I&T in Metastatic Castration-resistant Prostate Cancer. *Eur Urol*. 2019; 75: 920-6.
- Kratochwil C, Giesel FL, Stefanova M, Benešová M, Bronzel M, Afshar-Oromieh A, et al. PSMA-Targeted Radionuclide Therapy of Metastatic Castration-Resistant Prostate Cancer with <sup>177</sup>Lu-Labeled PSMA-617. *J Nucl Med*. 2016; 57: 1170-6.
- Rahbar K, Ahmadzadehfard H, Kratochwil C, Haberkorn U, Schäfers M, Essler M, et al. German Multicenter Study Investigating <sup>177</sup>Lu-PSMA-617 Radioligand Therapy in Advanced Prostate Cancer Patients. *J Nucl Med*. 2017; 58: 85-90.
- Hofman MS, Emmett L, Sandhu S, Irvani A, Joshua AM, Goh JC, et al. [<sup>177</sup>Lu]Lu-PSMA-617 versus cabazitaxel in patients with metastatic

- castration-resistant prostate cancer (TheraP): a randomised, open-label, phase 2 trial. *Lancet*. 2021; 397: 797-804.
27. Sartor O, de Bono J, Chi KN, Fizazi K, Herrmann K, Rahbar K, et al. Lutetium-177-PSMA-617 for Metastatic Castration-Resistant Prostate Cancer. *N Engl J Med*. 2021; 385: 1091-103.
  28. Yadav MP, Ballal S, Bal C, Sahoo RK, Damle NA, Tripathi M, Seth A. Efficacy and Safety of <sup>177</sup>Lu-PSMA-617 Radioligand Therapy in Metastatic Castration-Resistant Prostate Cancer Patients. *Clin Nucl Med*. 2020; 45: 19-31.
  29. Bu T, Zhang L, Yu F, Yao X, Wu W, Zhang P, et al. <sup>177</sup>Lu-PSMA-I&T Radioligand Therapy for Treating Metastatic Castration-Resistant Prostate Cancer: A Single-Centre Study in East Asians. *Front Oncol*. 2022; 12: 835956.
  30. Eiber M, Maurer T, Souvatzoglou M, Beer AJ, Ruffani A, Haller B, et al. Evaluation of Hybrid <sup>68</sup>Ga-PSMA Ligand PET/CT in 248 Patients with Biochemical Recurrence After Radical Prostatectomy. *J Nucl Med*. 2015; 56: 668-74.
  31. Rauscher I, Düwel C, Haller B, Rischpler C, Heck MM, Gschwend JE, et al. Efficacy, Predictive Factors, and Prediction Nomograms for <sup>68</sup>Ga-labeled Prostate-specific Membrane Antigen-ligand Positron-emission Tomography/Computed Tomography in Early Biochemical Recurrence Prostate Cancer After Radical Prostatectomy. *Eur Urol*. 2018; 73: 656-61.
  32. Lenzo NP, Meyrick D, Turner JH. Review of Gallium-68 PSMA PET/CT Imaging in the Management of Prostate Cancer. *Diagnostics (Basel)*. 2018; 8: 16.
  33. Maurer T, Robu S, Schottelius M, Schwamborn K, Rauscher I, van den Berg NS, et al. <sup>99m</sup>Tc-based Prostate-specific Membrane Antigen-radioligand Surgery in Recurrent Prostate Cancer. *Eur Urol*. 2019; 75: 659-66.
  34. Horn T, Krönke M, Rauscher I, Haller B, Robu S, Wester H-J, et al. Single Lesion on Prostate-specific Membrane Antigen-ligand Positron Emission Tomography and Low Prostate-specific Antigen Are Prognostic Factors for a Favorable Biochemical Response to Prostate-specific Membrane Antigen-targeted Radioligand Surgery in Recurrent Prostate Cancer. *Eur Urol*. 2019; 76: 517-23.
  35. Wurzer A, Di Carlo D, Schmidt A, Beck R, Eiber M, Schwaiger M, Wester HJ. Radiohybrid Ligands: A Novel Tracer Concept Exemplified by <sup>18</sup>F- or <sup>68</sup>Ga-Labeled rhPSMA Inhibitors. *J Nucl Med*. 2020; 61: 735-42.
  36. Eiber M, Kroenke M, Wurzer A, Ulbrich L, Jooß L, Maurer T, et al. <sup>18</sup>F-rhPSMA-7 PET for the Detection of Biochemical Recurrence of Prostate Cancer After Radical Prostatectomy. *J Nucl Med*. 2020; 61: 696-701.
  37. Gafita A, Fendler WP, Hui W, Sandhu S, Weber M, Esfandiari R, et al. Efficacy and Safety of (<sup>177</sup>)Lu-labeled Prostate-specific Membrane Antigen Radionuclide Treatment in Patients with Diffuse Bone Marrow Involvement: A Multicenter Retrospective Study. *Eur Urol*. 2020; 78: 148-54.
  38. Gafita A, Calais J, Grogan TR, Hadaschik B, Wang H, Weber M, et al. Nomograms to predict outcomes after (<sup>177</sup>)Lu-PSMA therapy in men with metastatic castration-resistant prostate cancer: an international, multicentre, retrospective study. *Lancet Oncol*. 2021; 22: 1115-25.
  39. Zacherl MJ, Gildehaus FJ, Mittlmeier L, Boening G, Gosewisch A, Wenter V, et al. First clinical results for PSMA targeted alpha therapy using <sup>225</sup>Ac-PSMA-I&T in advanced mCRPC patients. *J Nucl Med*. 2021; 62: 669-74.
  40. Feueracker B, Tauber R, Knorr K, Heck M, Beheshti A, Seidl C, et al. Activity and Adverse Events of Actinium-225-PSMA-617 in Advanced Metastatic Castration-resistant Prostate Cancer After Failure of Lutetium-177-PSMA. *Eur Urol*. 2021; 79: 343-50.
  41. Schottelius M, Osl T, Poschenrieder A, Hoffmann F, Beykan S, Häscheid H, et al. [<sup>177</sup>Lu]pentixather: Comprehensive Preclinical Characterization of a First CXCR4-directed Endoradiotherapeutic Agent. *Theranostics*. 2017; 7: 2350-62.
  42. Herrmann K, Schottelius M, Lapa C, Osl T, Poschenrieder A, Häscheid H, et al. First-in-Human Experience of CXCR4-Directed Endoradiotherapy with <sup>177</sup>Lu- and <sup>90</sup>Y-Labeled Pentixather in Advanced-Stage Multiple Myeloma with Extensive Intra- and Extramedullary Disease. *J Nucl Med*. 2016; 57: 248-51.
  43. Lapa C, Häscheid H, Kircher M, Schirbel A, Wunderlich G, Werner R, et al. Feasibility of CXCR4-directed radioligand therapy in advanced diffuse large B cell lymphoma. *J Nucl Med*. 2019; 60: 60-4.
  44. Xu J, Li S, Xu S, Dai J, Luo Z, Cui J, et al. Screening and Preclinical Evaluation of Novel Radiolabeled Anti-Fibroblast Activation Protein- $\alpha$  Recombinant Antibodies. *Cancer Biother Radiopharm*. 2023; 38: 726-37.
  45. Watabe T, Liu Y, Kaneda-Nakashima K, Shirakami Y, Lindner T, Ooe K, et al. Theranostics Targeting Fibroblast Activation Protein in the Tumor Stroma: <sup>64</sup>Cu- and <sup>225</sup>Ac-Labeled FAPI-04 in Pancreatic Cancer Xenograft Mouse Models. *J Nucl Med*. 2020; 61: 563-9.
  46. Ma H, Li F, Shen G, Pan L, Liu W, Liang R, et al. In vitro and in vivo evaluation of <sup>211</sup>At-labeled fibroblast activation protein inhibitor for glioma treatment. *Bioorg Med Chem*. 2022; 55: 116600.
  47. Liu Y, Watabe T, Kaneda-Nakashima K, Shirakami Y, Naka S, Ooe K, et al. Fibroblast activation protein targeted therapy using [<sup>177</sup>Lu]FAPI-46 compared with [<sup>225</sup>Ac]FAPI-46 in a pancreatic cancer model. *Eur J Nucl Med Mol Imaging*. 2022; 49: 871-80.
  48. Lindner T, Loktev A, Altmann A, Giesel F, Kratochwil C, Debus J, et al. Development of Quinoline-Based Theranostic Ligands for the Targeting of Fibroblast Activation Protein. *J Nucl Med*. 2018; 59: 1415-22.
  49. Ferdinandus J, Costa PF, Kessler L, Weber M, Hirmas N, Kostbade K, et al. Initial Clinical Experience with <sup>90</sup>Y-FAPI-46 Radioligand Therapy for Advanced-Stage Solid Tumors: A Case Series of 9 Patients. *J Nucl Med*. 2022; 63: 727-34.
  50. Baum RP, Schuchardt C, Singh A, Chantadisai M, Robiller FC, Zhang J, et al. Feasibility, Biodistribution, and Preliminary Dosimetry in Peptide-Targeted Radionuclide Therapy of Diverse Adenocarcinomas Using <sup>177</sup>Lu-FAP-2286: First-in-Humans Results. *J Nucl Med*. 2022; 63: 415-23.
  51. Zboralski D, Hoehne A, Bredenbeck A, Schumann A, Nguyen M, Schneider E, et al. Preclinical evaluation of FAP-2286 for fibroblast activation protein targeted radionuclide imaging and therapy. *Eur J Nucl Med Mol Imaging*. 2022; 49: 3651-67.
  52. Hallett RM, Poplawski SE, Dornan MH, Ahn SH, Pan S, Wengen W et al. Pre-clinical characterization of the novel Fibroblast Activation Protein (FAP) targeting ligand PNT6555 for the imaging and therapy of cancer[J/OL]. *Cancer Res* 2022; 82(Suppl 12): 3303.
  53. Reubi JC, Schär JC, Waser B, Wenger S, Heppeler A, Schmitt JS, Mäcke HR. Affinity profiles for human somatostatin receptor subtypes SST1-SST5 of somatostatin radiotracers selected for scintigraphic and radiotherapeutic use. *Eur J Nucl Med*. 2000; 27: 273-82.
  54. Fani M, Braun F, Waser B, Beetschen K, Cescato R, Erchevyi J, et al. Unexpected sensitivity of sst2 antagonists to N-terminal radiometal modifications. *J Nucl Med*. 2012; 53: 1481-9.
  55. Loktev A, Lindner T, Mier W, Debus J, Altmann A, Jäger D, et al. A Tumor-Imaging Method Targeting Cancer-Associated Fibroblasts. *J Nucl Med*. 2018; 59: 1423-9.
  56. Oomen SP, van Hennik PB, Antonissen C, Lichtenauer-Kaligis EG, Hofland LJ, Lamberts SW, et al. Somatostatin is a selective chemoattractant for primitive (CD34<sup>+</sup>) hematopoietic progenitor cells. *Exp Hematol*. 2002; 30: 116-25.
  57. Cheng H, Zheng Z, Cheng T. New paradigms on hematopoietic stem cell differentiation. *Protein Cell*. 2020; 11: 34-44.
  58. Tao Y, Jakobsson V, Chen X, Zhang J. Exploiting Albumin as a Versatile Carrier for Cancer Theranostics. *Acc Chem Res*. 2023; 56: 2403-15.
  59. Müller C, Struthers H, Winiger C, Zhernosekov K, Schibli R. DOTA conjugate with an albumin-binding entity enables the first folic acid-targeted <sup>177</sup>Lu-radionuclide tumor therapy in mice. *J Nucl Med*. 2013; 54: 124-31.
  60. Kelly J, Amor-Coarasa A, Ponnala S, Nikolopoulou A, Williams C, Schlyer D, et al. Trifunctional PSMA-targeting constructs for prostate cancer with unprecedented localization to LNCaP tumors. *Eur J Nucl Med Mol Imaging*. 2018; 45: 1841-51.
  61. Kelly JM, Amor-Coarasa A, Ponnala S, Nikolopoulou A, Clarence Williams J, DiMaggio SG, Babich JW. Albumin-Binding PSMA Ligands: Implications for Expanding the Therapeutic Window. *J Nucl Med*. 2019; 60: 656-63.
  62. Kuo H-T, Lin K-S, Zhang Z, Uribe CF, Merkens H, Zhang C, Bénard F. <sup>177</sup>Lu-Labeled Albumin-Binder-Conjugated PSMA-Targeting Agents with Extremely High Tumor Uptake and Enhanced Tumor-to-Kidney Absorbed Dose Ratio. *J Nucl Med*. 2021; 62: 521-7.
  63. Tschan VJ, Borgna F, Busslinger SD, Stirn M, Rodriguez JMM, Bernhardt P, et al. Preclinical investigations using [<sup>177</sup>Lu]Lu-Ibu-DAB-PSMA toward its clinical translation for radioligand therapy of prostate cancer. *Eur J Nucl Med Mol Imaging*. 2022; 49: 3639-50.
  64. Borgna F, Deberle LM, Busslinger SD, Tschan VJ, Walde LM, Becker AE, et al. Preclinical Investigations to Explore the Difference between the Diastereomers [<sup>177</sup>Lu]Lu-SibuDAB and [<sup>177</sup>Lu]Lu-RibuDAB toward Prostate Cancer Therapy. *Mol Pharm*. 2022; 19: 2105-14.
  65. Jeitner TM, Babich JW, Kelly JM. Advances in PSMA theranostics. *Transl Oncol*. 2022; 22: 101450.
  66. Umbrecht CA, Benešová M, Schibli R, Müller C. Preclinical Development of Novel PSMA-Targeting Radioligands: Modulation of Albumin-Binding Properties To Improve Prostate Cancer Therapy. *Mol Pharm*. 2018; 15: 2297-306.
  67. Wang Z, Tian R, Niu G, Ma Y, Lang L, Szajek LP, et al. Single Low-Dose Injection of Evans Blue Modified PSMA-617 Radioligand Therapy Eliminates Prostate-Specific Membrane Antigen Positive Tumors. *Bioconjug Chem*. 2018; 29: 3213-21.
  68. Zang J, Fan X, Wang H, Liu Q, Wang J, Li H, et al. First-in-human study of <sup>177</sup>Lu-EB-PSMA-617 in patients with metastatic castration-resistant prostate cancer. *Eur J Nucl Med Mol Imaging*. 2019; 46: 148-58.
  69. Zang J, Liu Q, Sui H, Wang R, Jacobson O, Fan X, et al. <sup>177</sup>Lu-EB-PSMA Radioligand Therapy with Escalating Doses in Patients with Metastatic Castration-Resistant Prostate Cancer. *J Nucl Med*. 2020; 61: 1772-8.
  70. Kramer V, Fernández R, Lehnert W, Jiménez-Franco LD, Soza-Ried C, Eppard E, et al. Biodistribution and dosimetry of a single dose of albumin-binding ligand [<sup>177</sup>Lu]Lu-PSMA-ALB-56 in patients with mCRPC. *Eur J Nucl Med Mol Imaging*. 2021; 48: 893-903.
  71. Wen X, Xu P, Zeng X, Liu J, Du C, Zeng X, et al. Development of [<sup>177</sup>Lu]Lu-LNC1003 for radioligand therapy of prostate cancer with a moderate level of PSMA expression. *Eur J Nucl Med Mol Imaging*. 2023; 50: 2846-60.
  72. Zang J, Wang G, Zhao T, Liu H, Lin X, Yang Y, et al. A phase 1 trial to determine the maximum tolerated dose and patient-specific dosimetry of [<sup>177</sup>Lu]Lu-LNC1003 in patients with metastatic castration-resistant prostate cancer. *Eur J Nucl Med Mol Imaging*. 2024; 51: 871-82.
  73. Jiang Y, Liu Q, Wang G, Sui H, Wang R, Wang J, et al. Safety and efficacy of peptide receptor radionuclide therapy with <sup>177</sup>Lu-DOTA-EB-TATE in patients with metastatic neuroendocrine tumors. *Theranostics*. 2022; 12: 6437-45.
  74. Müller C, Zhernosekov K, Köster U, Johnston K, Dorrer H, Hohn A, et al. A unique matched quadruplet of terbium radioisotopes for PET and SPECT and for  $\alpha$ - and  $\beta$ -radionuclide therapy: an in vivo proof-of-concept study with a new receptor-targeted folate derivative. *J Nucl Med*. 2012; 53: 1951-9.

75. Müller C, Singh A, Umbricht CA, Kulkarni HR, Johnston K, Benešová M, et al. Preclinical investigations and first-in-human application of <sup>152</sup>Tb-PSMA-617 for PET/CT imaging of prostate cancer. *EJNMMI Res.* 2019; 9: 68.
76. Baum RP, Singh A, Kulkarni HR, Bernhardt P, Rydén T, Schuchardt C, et al. First-in-Humans Application of (161)Tb: A Feasibility Study Using <sup>161</sup>Tb-DOTATOC. *J Nucl Med.* 2021; 62: 1391-7.
77. Eychemme R, Chérel M, Haddad F, Guérard F, Gestin JF. Overview of the Most Promising Radionuclides for Targeted Alpha Therapy: The "Hopeful Eight". *Pharmaceutics.* 2021; 13: 906.
78. Umbricht CA, Köster U, Bernhardt P, Gracheva N, Johnston K, Schibli R, et al. Alpha-PET for Prostate Cancer: Preclinical investigation using <sup>149</sup>Tb-PSMA-617. *Sci Rep.* 2019; 9: 17800.
79. Moiseeva AN, Aliev RA, Unezhev VN, Zagryadskiy VA, Latushkin ST, Akseonov NV, et al. Cross section measurements of <sup>151</sup>Eu(<sup>3</sup>He,5n) reaction: new opportunities for medical alpha emitter <sup>149</sup>Tb production. *Sci Rep.* 2020; 10: 508.
80. Aluicio-Sarduy E, Barnhart TE, Weichert J, Hernandez R, Engle JW. Cyclotron-Produced <sup>132</sup>La as a PET Imaging Surrogate for Therapeutic <sup>225</sup>Ac. *J Nucl Med.* 2021; 62: 1012-5.
81. Fan W, Yung B, Huang P, Chen X. Nanotechnology for Multimodal Synergistic Cancer Therapy. *Chem Rev.* 2017; 117: 13566-638.
82. Li X, Lovell JF, Yoon J, Chen X. Clinical development and potential of photothermal and photodynamic therapies for cancer. *Nat Rev Clin Oncol.* 2020; 17: 657-74.
83. Bertrand N, Wu J, Xu X, Kamaly N, Farokhzad OC. Cancer nanotechnology: the impact of passive and active targeting in the era of modern cancer biology. *Adv Drug Deliv Rev.* 2014; 66: 2-25.
84. Chen H, Zhang W, Zhu G, Xie J, Chen X. Rethinking cancer nanotheranostics. *Nat Rev Mater.* 2017; 2.
85. Karimi M, Ghasemi A, Sahandi Zangabad P, Rahighi R, Moosavi Basri SM, Mirshekari H, et al. Smart micro/nanoparticles in stimulus-responsive drug/gene delivery systems. *Chem Soc Rev.* 2016; 45: 1457-501.
86. Cheng J, Zhu Y, Dai Y, Li L, Zhang M, Jin D, et al. Gas-Mediated Tumor Energy Remodeling for Sensitizing Mild Photothermal Therapy. *Angew Chem Int Ed Engl.* 2023; 62: e202304312.
87. Tang W, Yang Z, He L, Deng L, Fathi P, Zhu S, et al. A hybrid semiconducting organosilica-based O<sub>2</sub> nanoeconomizer for on-demand synergistic photothermally boosted radiotherapy. *Nat Commun.* 2021; 12: 523.
88. Bhatia SN, Chen X, Dobrovolskaia MA, Lammers T. Cancer nanomedicine. *Nat Rev Cancer.* 2022; 22: 550-6.
89. Gao Z, Jia S, Ou H, Hong Y, Shan K, Kong X, et al. An Activatable Near-Infrared Afterglow Theranostic Prodrug with Self-Sustainable Magnification Effect of Immunogenic Cell Death. *Angew Chem Int Ed Engl.* 2022; 61: e202209793.
90. Zhu J, Zhang Y, Li Z, Bao X, Zhou Y, Ma B, et al. Tumor-microenvironment-responsive poly-prodrug encapsulated semiconducting polymer nanosystem for phototherapy-boosted chemotherapy. *Mater Horiz.* 2023; 10: 3014-23.
91. Jia R, Xu H, Wang C, Su L, Jing J, Xu S, et al. NIR-II emissive AIEgen photosensitizers enable ultrasensitive imaging-guided surgery and phototherapy to fully inhibit orthotopic hepatic tumors. *J Nanobiotechnology.* 2021; 19: 419.
92. Pei P, Chen Y, Sun C, Fan Y, Yang Y, Liu X, et al. X-ray-activated persistent luminescence nanomaterials for NIR-II imaging. *Nat Nanotechnol.* 2021; 16: 1011-8.
93. Wang T, Wang S, Liu Z, He Z, Yu P, Zhao M, et al. A hybrid erbium(III)-bacteriochlorin near-infrared probe for multiplexed biomedical imaging. *Nat Mater.* 2021; 20: 1571-8.
94. Xu Y, Li C, Xu R, Zhang N, Wang Z, Jing X, et al. Tuning molecular aggregation to achieve highly bright AIE dots for NIR-II fluorescence imaging and NIR-I photoacoustic imaging. *Chem Sci.* 2020; 11: 8157-66.
95. An J, Tang S, Hong G, Chen W, Chen M, Song J, et al. An unexpected strategy to alleviate hypoxia limitation of photodynamic therapy by biotinylation of photosensitizers. *Nat Commun.* 2022; 13: 2225.
96. Ayan S, Gunaydin G, Yesilgul-Mehmetcik N, Gedik ME, Seven O, Akkaya EU. Proof-of-principle for two-stage photodynamic therapy: hypoxia triggered release of singlet oxygen. *Chem Commun (Camb).* 2020; 56: 14793-6.
97. Cheng Y, Cheng H, Jiang C, Qiu X, Wang K, Huan W, et al. Perfluorocarbon nanoparticles enhance reactive oxygen levels and tumour growth inhibition in photodynamic therapy. *Nat Commun.* 2015; 6: 8785.
98. de Haas ER, de Vijlder HC, Sterenborg HJ, Neumann HA, Robinson DJ. Fractionated aminolevulinic acid-photodynamic therapy provides additional evidence for the use of PDT for non-melanoma skin cancer. *J Eur Acad Dermatol Venereol.* 2008; 22: 426-30.
99. Koleman S, Ozdemir T, Lee D, Kim GM, Karatas T, Yoon J, Akkaya EU. Remote-Controlled Release of Singlet Oxygen by the Plasmonic Heating of Endoperoxide-Modified Gold Nanorods: Towards a Paradigm Change in Photodynamic Therapy. *Angew Chem Int Ed Engl.* 2016; 55: 3606-10.
100. Middelburg TA, de Bruijn HS, van der Ploeg-van den Heuvel A, Neumann HA, Robinson DJ. The effect of light fractionation with a 2-h dark interval on the efficacy of topical hexyl-aminolevulinic photodynamic therapy in normal mouse skin. *Photodiagnosis Photodyn Ther.* 2013; 10: 703-9.
101. Turan IS, Yildiz D, Turksoy A, Gunaydin G, Akkaya EU. A Bifunctional Photosensitizer for Enhanced Fractional Photodynamic Therapy: Singlet Oxygen Generation in the Presence and Absence of Light. *Angew Chem Int Ed Engl.* 2016; 55: 2875-8.
102. Wang W, Cheng Y, Yu P, Wang H, Zhang Y, Xu H, et al. Perfluorocarbon regulates the intratumoural environment to enhance hypoxia-based agent efficacy. *Nat Commun.* 2019; 10: 1580.
103. Xiao Z, Halls S, Dickey D, Tulip J, Moore RB. Fractionated versus standard continuous light delivery in interstitial photodynamic therapy of dunning prostate carcinomas. *Clin Cancer Res.* 2007; 13: 7496-505.
104. Zou J, Li L, Zhu J, Li X, Yang Z, Huang W, Chen X. Singlet Oxygen "Afterglow" Therapy with NIR-II Fluorescent Molecules. *Adv Mater.* 2021; 33: e2103627.
105. Chen K, He P, Wang Z, Tang BZ. A Feasible Strategy of Fabricating Type I Photosensitizer for Photodynamic Therapy in Cancer Cells and Pathogens. *ACS Nano.* 2021; 15: 7735-43.
106. Ding H, Yu H, Dong Y, Tian R, Huang G, Boothman DA, et al. Photoactivation switch from type II to type I reactions by electron-rich micelles for improved photodynamic therapy of cancer cells under hypoxia. *J Control Release.* 2011; 156: 276-80.
107. Gilson RC, Black KCL, Lane DD, Achilefu S. Hybrid TiO<sub>2</sub> -Ruthenium Nano-photosensitizer Synergistically Produces Reactive Oxygen Species in both Hypoxic and Normoxic Conditions. *Angew Chem Int Ed Engl.* 2017; 56: 10717-20.
108. Kang M, Zhang Z, Xu W, Wen H, Zhu W, Wu Q, et al. Good Steel Used in the Blade: Well-Tailored Type-I Photosensitizers with Aggregation-Induced Emission Characteristics for Precise Nuclear Targeting Photodynamic Therapy. *Adv Sci (Weinh).* 2021; 8: e2100524.
109. Lan G, Ni K, Veroneau SS, Feng X, Nash GT, Luo T, et al. Titanium-Based Nanoscale Metal-Organic Framework for Type I Photodynamic Therapy. *J Am Chem Soc.* 2019; 141: 4204-8.
110. Li X, Lee D, Huang JD, Yoon J. Phthalocyanine-Assembled Nanodots as Photosensitizers for Highly Efficient Type I Photoreactions in Photodynamic Therapy. *Angew Chem Int Ed Engl.* 2018; 57: 9885-90.
111. Wang Y-Y, Liu Y-C, Sun H, Guo D-S. Type I photodynamic therapy by organic-inorganic hybrid materials: From strategies to applications. *Coord Chem Rev.* 2019; 395: 46-62.
112. Zou J, Zhu J, Yang Z, Li L, Fan W, He L, et al. A Phototheranostic Strategy to Continuously Deliver Singlet Oxygen in the Dark and Hypoxic Tumor Microenvironment. *Angew Chem Int Ed Engl.* 2020; 59: 8833-8.
113. Chen Z, Liu W, Yang Z, Luo Y, Qiao C, Xie A, et al. Sonodynamic-immunomodulatory nanostimulators activate pyroptosis and remodel tumor microenvironment for enhanced tumor immunotherapy. *Theranostics.* 2023; 13: 1571-83.
114. Duan Y, Yu Y, Liu P, Gao Y, Dai X, Zhang L, et al. Reticular Chemistry-Enabled Sonodynamic Activity of Covalent Organic Frameworks for Nanodynamic Cancer Therapy. *Angew Chem Int Ed Engl.* 2023; 62: e202302146.
115. Gao C, Kwong CHT, Wang Q, Kam H, Xie B, Lee SM, et al. Conjugation of Macrophage-Mimetic Microalgae and Liposome for Antitumor Sonodynamic Immunotherapy via Hypoxia Alleviation and Autophagy Inhibition. *ACS Nano.* 2023; 17: 4034-49.
116. Gong M, Huang Y, Feng H, Lin J, Huang A, Hu J, et al. A nanodrug combining CD47 and sonodynamic therapy efficiently inhibits osteosarcoma deterioration. *J Control Release.* 2023; 355: 68-84.
117. Jiang S, Liu C, He Q, Dang K, Zhang W, Tian Y. Porphyrin-based metal-organic framework nanocrystals for combination of immune and sonodynamic therapy. *Nano Res.* 2023; 16: 9633-41.
118. Zhou L, Lyu J, Liu F, Su Y, Feng L, Zhang X. Immunogenic PANoptosis-Initiated Cancer Sono-Immune Reediting Nanotherapy by Iteratively Boosting Cancer Immunity Cycle. *Adv Mater.* 2023; e2305361.
119. Li Y, Lu N, Lin Q, Wang H, Liang Z, Lu Y, Zhang P. Sono-ReCORMs for synergistic sonodynamic-gas therapy of hypoxic tumor. *Chin Chem Lett.* 2023; 34: 107653.
120. Song K, Chen G, He Z, Shen J, Ping J, Li Y, et al. Protoporphyrin-sensitized degradable bismuth nanoformulations for enhanced sonodynamic oncotherapy. *Acta Biomater.* 2023; 158: 637-48.
121. Sun Y, Wang Y, Han R, Ren Z, Chen X, Dong W, et al. Ultrasound cascade regulation of nano-oxygen hybrids triggering ferroptosis augmented sonodynamic anticancer therapy. *Nano Res.* 2023; 16: 7280-92.
122. Wang L, Mao Z, Wu J, Cui X, Wang Y, Yang N, et al. Engineering layered double hydroxide-based sonocatalysts for enhanced sonodynamic-immunotherapy. *Nano Today.* 2023; 49: 101782.
123. Wu W, Xu M, Qiao B, Huang T, Guo H, Zhang N, et al. Nanodroplet-enhanced sonodynamic therapy potentiates immune checkpoint blockade for systemic suppression of triple-negative breast cancer. *Acta Biomater.* 2023; 158: 547-59.
124. Xu C, Huang J, Jiang Y, He S, Zhang C, Pu K. Nanoparticles with ultrasound-induced afterglow luminescence for tumour-specific theranostics. *Nat Biomed Eng.* 2023; 7: 298-312.
125. Zhou L, Feng W, Mao Y, Chen Y, Zhang X. Nanoengineered sonosensitive platelets for synergistically augmented sonodynamic tumor therapy by glutamine deprivation and cascading thrombosis. *Bioact Mater.* 2023; 24: 26-36.
126. Du Y, Liu D, Sun M, Shu G, Qi J, You Y, et al. Multifunctional Gd-CuS loaded UCST polymeric micelles for MR/PA imaging-guided chemo-photothermal tumor treatment. *Nano Res.* 2021; 15: 2288-99.

127. Kumar R, Srivastava VR, Mahapatra S, Dkhar DS, Kumari R, Prerna K, et al. Drug Encapsulated Lipid-Polymeric Nanohybrid as a Chemo-therapeutic Platform of Cancer. *Nanotheranostics*. 2023; 7: 167-75.
128. Li Y, Kong J, Zhao H, Liu Y. Synthesis of Multi-Stimuli Responsive Fe<sub>3</sub>O<sub>4</sub> Coated with Diamonds Nanocomposite for Magnetic Assisted Chemo-Photothermal Therapy. *Molecules*. 2023; 28: 1784.
129. Lu F, Sang R, Tang Y, Xia H, Liu J, Huang W, et al. Fabrication of a phototheranostic nanopatform for single laser-triggered NIR-II fluorescence imaging-guided photothermal/chemo/antiangiogenic combination therapy. *Acta Biomater*. 2022; 151: 528-36.
130. Palange AL, Mascolo DD, Ferreira M, Gawne PJ, Spano R, Felici A, et al. Boosting the Potential of Chemotherapy in Advanced Breast Cancer Lung Metastasis via Micro-Combinatorial Hydrogel Particles. *Adv Sci (Weinh)*. 2023; 10: e2205223.
131. Shi Y, Zhou M, Zhang Y, Wang Y, Cheng J. MRI-guided dual-responsive anti-tumor nanostructures for synergistic chemo-photothermal therapy and chemodynamic therapy. *Acta Biomater*. 2023; 158: 571-82.
132. Wu Y, Chen S, Zhu J. Hydrogen Bond-Mediated Supramolecular Polymeric Nanomedicine with pH/Light-Responsive Methotrexate Release and Synergistic Chemo-/Photothermal Therapy. *Biomacromolecules*. 2022; 23: 4230-40.
133. Yang R, Ouyang Z, Guo H, Qu J, Xia J, Shen M, Shi X. Microfluidic synthesis of intelligent nanoclusters of ultrasmall iron oxide nanoparticles with improved tumor microenvironment regulation for dynamic MR imaging-guided tumor photothermo-chemo-chemodynamic therapy. *Nano Today*. 2022; 46: 101615.
134. Yang R, Zhan M, Ouyang Z, Guo H, Qu J, Xia J, et al. Microfluidic synthesis of fibronectin-coated polydopamine nanocomplexes for self-supplementing tumor microenvironment regulation and MR imaging-guided chemo-chemodynamic-immune therapy. *Mater Today Bio*. 2023; 20: 100670.
135. Zhang R, Hao L, Chen P, Zhang G, Liu N. Multifunctional small-molecule theranostic agents for tumor-specific imaging and targeted chemotherapy. *Bioorg Chem*. 2023; 137: 106576.
136. Zhang X, Ge Y, Liu M, Pei Y, He P, Song W, Zhang S. DNA-Au Janus Nanoparticles for In Situ SERS Detection and Targeted Chemo-photodynamic Synergistic Therapy. *Anal Chem*. 2022; 94: 7823-32.
137. Zhang Z, Zhang K, Wang R, Zhu J, Xue J, Liu F, et al. A self-amplified necrotic targeting theranostic nanoparticle with deep tumor penetration for imaging-guided personalized chemo-photodynamic therapy. *Chem Eng J*. 2023; 455: 140465.
138. Chen S, Zhong Y, Fan W, Xiang J, Wang G, Zhou Q, et al. Enhanced tumor penetration and prolonged circulation in blood of polyzwitterion-drug conjugates with cell-membrane affinity. *Nat Biomed Eng*. 2021; 5: 1019-37.
139. Deng H, Zhou Z, Yang W, Lin LS, Wang S, Niu G, et al. Endoplasmic Reticulum Targeting to Amplify Immunogenic Cell Death for Cancer Immunotherapy. *Nano Lett*. 2020; 20: 1928-33.
140. Gheibi Hayat SM, Darroudi M. Nanovaccine: A novel approach in immunization. *J Cell Physiol*. 2019; 234: 12530-6.
141. Gong N, Zhang Y, Teng X, Wang Y, Huo S, Qing G, et al. Proton-driven transformable nanovaccine for cancer immunotherapy. *Nat Nanotechnol*. 2020; 15: 1053-64.
142. Liu C, Liu X, Xiang X, Pang X, Chen S, Zhang Y, et al. A nanovaccine for antigen self-presentation and immunosuppression reversal as a personalized cancer immunotherapy strategy. *Nat Nanotechnol*. 2022; 17: 531-40.
143. Nguyen HT, Byeon JH, Phung CD, Pham LM, Ku SK, Yong CS, Kim JO. Method for the Instant In-Flight Manufacture of Black Phosphorus to Assemble Core@Shell Nanocomposites for Targeted Photoimmunotherapy. *ACS Appl Mater Interfaces*. 2019; 11: 24959-70.
144. Rao L, Wu L, Liu Z, Tian R, Yu G, Zhou Z, et al. Hybrid cellular membrane nanovesicles amplify macrophage immune responses against cancer recurrence and metastasis. *Nat Commun*. 2020; 11: 4909.
145. Rao L, Zhao SK, Wen C, Tian R, Lin L, Cai B, et al. Activating Macrophage-Mediated Cancer Immunotherapy by Genetically Edited Nanoparticles. *Adv Mater*. 2020; 32: e2004853.
146. Xu J, Lv J, Zhuang Q, Yang Z, Cao Z, Xu L, et al. A general strategy towards personalized nanovaccines based on fluoropolymers for post-surgical cancer immunotherapy. *Nat Nanotechnol*. 2020; 15: 1043-52.
147. Fan W, Huang P, Chen X. Overcoming the Achilles' heel of photodynamic therapy. *Chem Soc Rev*. 2016; 45: 6488-519.
148. Liu Y, Bhattarai P, Dai Z, Chen X. Photothermal therapy and photoacoustic imaging via nanotheranostics in fighting cancer. *Chem Soc Rev*. 2019; 48: 2053-108.
149. Zhou Z, Song J, Nie L, Chen X. Reactive oxygen species generating systems meeting challenges of photodynamic cancer therapy. *Chem Soc Rev*. 2016; 45: 6597-626.
150. Liu Y, Li Y, Koo S, Sun Y, Liu Y, Liu X, et al. Versatile Types of Inorganic/Organic NIR-IIa/IIb Fluorophores: From Strategic Design toward Molecular Imaging and Theranostics. *Chem Rev*. 2022; 122: 209-68.
151. Li H, Wang X, Ohulchanskyy TY, Chen G. Lanthanide-Doped Near-Infrared Nanoparticles for Biophotonics. *Adv Mater*. 2021; 33: e2000678.
152. Xu W, Wang D, Tang BZ. NIR-II AIEgens: A Win-Win Integration towards Bioapplications. *Angew Chem Int Ed Engl*. 2021; 60: 7476-87.
153. Zhang NN, Lu CY, Chen MJ, Xu XL, Shu GF, Du YZ, Ji JS. Recent advances in near-infrared II imaging technology for biological detection. *J Nanobiotechnology*. 2021; 19: 132.
154. Li J, Zhuang Z, Zhao Z, Tang BZ. Type I AIE photosensitizers: Mechanism and application. *View*. 2021; 3: 20200121.
155. Lin H, Chen Y, Shi J. Nanoparticle-triggered in situ catalytic chemical reactions for tumour-specific therapy. *Chem Soc Rev*. 2018; 47: 1938-58.
156. Zhou J, Yu G, Huang F. Supramolecular chemotherapy based on host-guest molecular recognition: a novel strategy in the battle against cancer with a bright future. *Chem Soc Rev*. 2017; 46: 7021-53.
157. Yang F, Dong J, Li Z, Wang Z. Metal-Organic Frameworks (MOF)-Assisted Sonodynamic Therapy in Anticancer Applications. *ACS Nano*. 2023; 17: 4102-33.
158. Syed HR, Kilburn L, Fonseca A, Nazarian J, Oluigbo C, Myseros JS, et al. First-in-human sonodynamic therapy with ALA for pediatric diffuse intrinsic pontine glioma: a phase 1/2 study using low-intensity focused ultrasound : Technical communication. *J Neurooncol*. 2023; 162: 449-51.
159. Zha B, Yang J, Dang Q, Li P, Shi S, Wu J, et al. A phase I clinical trial of sonodynamic therapy combined with temozolomide in the treatment of recurrent glioblastoma. *J Neurooncol*. 2023; 162: 317-26.
160. Zhu L, Li Y, Jiang M, Ke C, Long H, Qiu M, et al. Self-Assembly of Precisely Fluorinated Albumin for Dual Imaging-Guided Synergistic Chemo-Photothermal-Photodynamic Cancer Therapy. *ACS Appl Mater Interfaces*. 2023; 15: 2665-78.
161. Sang W, Zhang Z, Dai Y, Chen X. Recent advances in nanomaterial-based synergistic combination cancer immunotherapy. *Chem Soc Rev*. 2019; 48: 3771-810.
162. Zhang C, Pu K. Molecular and nanoengineering approaches towards activatable cancer immunotherapy. *Chem Soc Rev*. 2020; 49: 4234-53.
163. Zhang X, Yang B, Ni Q, Chen X. Materials engineering strategies for cancer vaccine adjuvant development. *Chem Soc Rev*. 2023; 52: 2886-910.
164. Li Z, Zou J, Chen X. In Response to Precision Medicine: Current Subcellular Targeting Strategies for Cancer Therapy. *Adv Mater*. 2023; 35: e2209529.
165. Shi C, Zhang Q, Yao Y, Zeng F, Du C, Nijjati S, et al. Targeting the activity of T cells by membrane surface redox regulation for cancer theranostics. *Nat Nanotechnol*. 2023; 18: 86-97.
166. Zhu G, Mei L, Vishwasrao HD, Jacobson O, Wang Z, Liu Y, et al. Intertwining DNA-RNA nanocapsules loaded with tumor neoantigens as synergistic nanovaccines for cancer immunotherapy. *Nat Commun*. 2017; 8: 1482.
167. Cameron DE, Bashor CJ, Collins JJ. A brief history of synthetic biology. *Nat Rev Microbiol*. 2014.
168. Ruder WC, Lu T, Collins JJ. Synthetic biology moving into the clinic. *Science*. 2011; 333: 1248-52.
169. Jackson DA, Symons RH, Berg P. Biochemical method for inserting new genetic information into DNA of Simian Virus 40: circular SV40 DNA molecules containing lambda phage genes and the galactose operon of *Escherichia coli*. *Proc Natl Acad Sci U S A*. 1972; 69: 2904-9.
170. Gilad AA, Shapiro MG. Molecular Imaging in Synthetic Biology, and Synthetic Biology in Molecular Imaging. *Mol Imaging Biol*. 2017; 19: 373-8.
171. Aghi M, Hochberg F, Breakefield XO. Prodrug activation enzymes in cancer gene therapy. *J Gene Med*. 2000; 2: 148-64.
172. Porter DJT. *Escherichia coli* cytosine deaminase: the kinetics and thermodynamics for binding of cytosine to the apoenzyme and the Zn<sup>2+</sup> holoenzyme are similar. *Biochim Biophys Acta*. 2000; 1476: 239-52.
173. Liu G, Liang Y, Bar-Shir A, Chan KW, Galporthawela CS, Bernard SM, et al. Monitoring enzyme activity using a diamagnetic chemical exchange saturation transfer magnetic resonance imaging contrast agent. *J Am Chem Soc*. 2011; 133: 16326-9.
174. Singh RK, Lee JK, Selvaraj C, Singh R, Li J, Kim SY, Kalia VC. Protein Engineering Approaches in the Post-Genomic Era. *Curr Protein Pept Sci*. 2018; 19: 5-15.
175. Li C, Zhang R, Wang J, Wilson LM, Yan Y. Protein Engineering for Improving and Diversifying Natural Product Biosynthesis. *Trends Biotechnol*. 2020; 38: 729-44.
176. Engqvist MKM, Rabe KS. Applications of Protein Engineering and Directed Evolution in Plant Research. *Plant Physiol*. 2019; 179: 907-17.
177. Baek M, DiMaio F, Anishchenko I, Dauparas J, Ovchinnikov S, Lee GR, et al. Accurate prediction of protein structures and interactions using a three-track neural network. *Science*. 2021; 373: 871-6.
178. Jumper J, Evans R, Pritzel A, Green T, Figurnov M, Ronneberger O, et al. Highly accurate protein structure prediction with AlphaFold. *Nature*. 2021; 596: 583-9.
179. Lee HD, Grady CJ, Krell K, Strebeck C, Good NM, Martinez-Gomez NC, Gilad AA. A Novel Protein for the Bioremediation of Gadolinium Waste. *bioRxiv*. 2023: 2023.01.05.522788.
180. Romei MG, Boxer SG. Split Green Fluorescent Proteins: Scope, Limitations, and Outlook. *Annu Rev Biophys*. 2019; 48: 19-44.
181. Farhana J, Hossain MN, Suzuki K, Matsuda T, Nagai T. Genetically Encoded Fluorescence/Bioluminescence Bimodal Indicators for Ca<sup>2+</sup> Imaging. *ACS Sensors*. 2019; 4: 1825-34.
182. Petersen ED, Lapan AP, Fillion AJ, Crespo EL, Lambert GG, Zanca AT, et al. Bioluminescent Genetically Encoded Glutamate Indicator for Molecular Imaging of Neuronal Activity. *ACS Synth Biol*. 2023; 12: 2301-9.
183. Ikefuama EC, Kendziorski GE, Anderson K, Shafar L, Prakash M, Hochgeschwender U, et al. Improved Locomotor Recovery in a Rat Model of Spinal Cord Injury by BioLuminescent-OptoGenetic (BL-OG) Stimulation with an Enhanced Luminopsin. *Int J Mol Sci*. 2022; 23: 12994.

184. Massoud TF, Paulmurugan R, Gambhir SS. A molecularly engineered split reporter for imaging protein-protein interactions with positron emission tomography. *Nat Med.* 2010; 16: 921-6.
185. Naisbett-Jones LC, Lohmann KJ. Magnetoreception and magnetic navigation in fishes: a half century of discovery. *J Comp Physiol A Neuroethol Sens Neural Behav Physiol.* 2022; 208: 19-40.
186. Warrant EJ. Unravelling the enigma of bird magnetoreception. *Nature.* 2021; 594: 497-8.
187. Krishnan V, Park SA, Shin SS, Alon L, Tressler CM, Stokes W, et al. Wireless control of cellular function by activation of a novel protein responsive to electromagnetic fields. *Sci Rep.* 2018; 8: 8764.
188. Ricker B, Mitra S, Castellanos EA, Grady CJ, Woldring D, Pelled G, Gilad AA. Proposed three-phenylalanine motif involved in magnetoreception signalling of an Actinopterygii protein expressed in mammalian cells. *Open Biol.* 2023; 13: 230019.
189. Grady CJ, Schossau J, Ashbaugh RC, Pelled G, Gilad AA. A putative design for electromagnetic activation of split proteins for molecular and cellular manipulation. *Front Bioeng Biotechnol.* 2024, doi: 10.3389/fbioe.2024.1355915
190. Serganova I, Ponomarev V, Blasberg R. Human reporter genes: potential use in clinical studies. *Nucl Med Biol.* 2007; 34: 791-807.
191. Bar-Shir A, Liu G, Liang Y, Yadav NN, McMahon MT, Walczak P, et al. Transforming thymidine into a magnetic resonance imaging probe for monitoring gene expression. *J Am Chem Soc.* 2013; 135: 1617-24.
192. Bar-Shir A, Bulte JW, Gilad AA. Molecular Engineering of Nonmetallic Biosensors for CEST MRI. *ACS Chem Biol.* 2015; 10: 1160-70.
193. Allouche-Arnon H, Khersonsky O, Tirukoti ND, Peleg Y, Dym O, Albeck S, et al. Computationally designed dual-color MRI reporters for noninvasive imaging of transgene expression. *Nat Biotechnol.* 2022; 40: 1143-9.
194. Solomon LD. *Synthetic Biology: Science, Business, and Policy.* Routledge; 2017.
195. Mader N, Nguyen Ngoc C, Kirkgöze B, Baumgarten J, Groener D, Klimek K, et al. Extended therapy with [<sup>177</sup>Lu]Lu-PSMA-617 in responding patients with high-volume metastatic castration-resistant prostate cancer. *Eur J Nucl Med Mol Imaging.* 2023; 50: 1811-21.